

Atmospheric and Oceanic Sciences
Forrestal Campus, Princeton University
NOAA Geophysical Fluid Dynamics Laboratory
Email: bpu@princeton.edu

Professor Philip Stier
Atmospheric Physics
Clarendon Laboratory
University of Oxford
Parks Road
Oxford
OX1 3PU

June 14th, 2018

Dear Editor Stier,

We have submitted a revised paper entitled “How reliable are CMIP5 models in simulating dust optical depth?” by B. Pu and P. Ginoux for consideration for *Atmospheric Chemistry and Physics*. The helpful comments from the two anonymous reviewers are sincerely appreciated. Our replies to each reviewer’s comments are attached. We also made some edits in the manuscript.

We gratefully appreciate your time and consideration!

Sincerely,

Bing Pu and Paul Ginoux

Interactive comment on “How reliable are CMIP5 models in simulating dust optical depth?” by Bing Pu and Paul Ginoux
Anonymous Referee #1

We thank the reviewer for very helpful comments. We reply to your comment (in *Italic*) below.

This work examines the performance of seven CMIP5 climate models with interactive dust emissions schemes against dust optical depth (DOD) from MODIS Deep Blue aerosol products. The performance assessment to reproduce magnitude, spatial pattern and variations of observed DOD is conducted in nine regions, namely North Africa, Middle East, Northern China, North America, India, Southeastern Asia, South Africa, South America and Australia. Furthermore, interannual variations of DOD are also examined together with the impact on it of controlling factors such as 10 m surface wind, precipitation and surface bareness derived from leaf area index (LAI) data. In order to examine the relative contribution of these controlling factors to DOD multiple linear regression is applied on both, observations and models. Calculated regression coefficients in addition to observed and simulated controlling factors are then used to project DOD to the future (both observations and models).

The authors show that although the models can reproduce the global distribution of DOD over land under present conditions, with a better representation over northern than southern hemisphere, the interannual variability of DOD is all in all not well captured by CMIP5 models. Furthermore, models also do not reproduce the observed relations between the DOD and the examined controlling factors. Projected changes of CMIP5 model mean under the RCP8.5 scenario are presented and compared to projections of a regression model.

The research presented is interesting and the paper is well written. As the authors mention in their introduction, performance of CMIP5 models to simulate dust has received little attention and this work is a good first step to change this. I recommend this paper to be published in ACP after some comments have been addressed.

General Comments:

1. The authors highlight the importance of examining the performance of current climate models in simulating dust and they choose to assess this performance by evaluating simulated DOD. In fact, in lines 73-75 the authors claim that evaluating DOD in “CMIP5 models will provide a clear picture of model capability of dust simulation”. Although optical depth is a very common variable when it comes to validate models with respect to aerosols (be it dust or any other species), it is an integrated variable and therefore it does not provide any insight into the performance to reproduce the vertical distribution of aerosols. It has been shown that regional and global dust models can present similar performance in simulating AOD but present large diversity in emissions, deposition, surface concentration and vertical distribution (Huneeus et al., 2016). Although that study refers to forecast application, it is consistent with the findings in Huneeus et al. (2011). The authors should acknowledge this limitation in the discussion or conclusions, that although this evaluation is informative and necessary, it does not provide a full picture of current climate models to simulate dust. This similar

performance in optical depth compared to large diversity in other parameters such as emissions, deposition and surface concentration might be linked to the practice to use AOD to tune dust simulations. Is this a practice that is also used in climate models?

We thank the reviewer for pointing out that DOD cannot provide a full picture of dust modeling skill by CMIP5 models. We modified lines 75-77: “A comprehensive evaluation of the climatology and interannual variation of global dust optical depth (DOD) in CMIP5 models will provide insights into models’ capability of simulating the integrated aerosol extinction due to dust, which is one of the key variables that determine radiative forcing of dust to the climate system.” and lines 604-609: “Since DOD is an integrated variable, it does not reflect the vertical distribution of dust aerosols. As pointed by Huneus et al., (2016), dust models with similar performance in simulating aerosol optical depth may have quite large differences in simulating vertical distribution, emission, deposition, and surface concentration of dust. An overall evaluation of dust modeling capability will require detailed examination of these variables and the life cycle of dust in CMIP5 models in addition to DOD.” to better address this issue.

We agree with the reviewer that the similar performance of models in simulating DOD versus their discrepancies in simulating variables such as surface concentration, emission, and deposition may be due to the fact that DOD or AOD is used to tune dust models. Same tuning method may be used in the climate models, too, and thus adds to the need to examine other variables related to dust life cycle in the CMIP5 models.

2. In addition to examining the DOD projections from CMIP5 models, the authors also project DOD using calculated regression coefficients and compare these results to the simulated ones. I have to admit that I have difficulties in seeing the usefulness of this exercise. What is the point of it?

The reason to provide a future DOD projection by the regression model in addition to CMIP5 models’ projection was not clearly addressed in the previous version. We added lines 513-522 to better explain the purpose of this analysis: “Here we also present the projected change of DOD from the regression model in Figure 9. The regression model (see section 2.4 for details) is developed based on observed relationships between MODIS DOD and local controlling factors and can largely capture the interannual variations of DOD in the present-day climate (Table S1 in the Supplement). Assuming that the observed connection between DOD and these controlling factors do not change dramatically in the future, we can use this regression model and CMIP5-model projected change of controlling factors to project DOD variations. Compared to DOD projection from CMIP5 models, this approach utilizes additionally observational constrains and is likely to provide a more reliable future projection.”

The authors state that similarities are found between both projections “which may be informative” without specifying for what they might be informative. What do differences and similarities of both projections tell us?

We removed “which may be informative”, and modified the sentence to: “we find some similarities between the two, which adds to the confidence of projected DOD change in these regions...” (lines 690-691). Although CMIP5 models overestimate the

influence of surface wind and precipitation and underestimate the role of bareness, there are some similarities between model and observations over regions such as North Africa in DJF and parts of the Arabian Peninsula in JJA (Fig. 6; lines 450-462), which indicate that models partially capture the connection between the DOD and these controlling factors in some regions. Therefore, the projection of DOD from CMIP5 models (Fig. 7) is not completely unreliable. The similarity between CMIP5 projection and the projection from the regression model thus adds to the confidence of projected change of DOD over North Africa, the Arabian Peninsula, and northern China in some seasons.

3. The authors could improve the description of the methodology applied in the study. Regression coefficients are computed by regressing DOD from MODIS onto the observed controlling factors, the same procedure is repeated with model outputs to obtain “model” regression factors. Now when the interannual variability is examined, in line 320 it is unclear whether the reconstructed DOD using model regression factors or the one based on observations. I would have thought the former but then lines 332-335 refer to the observations making me doubt what reconstruction is then used in the analysis.

The regression coefficients are derived from observations. We modified section 2.4 in the methodology section and lines 412-414 to improve the clarity.

Furthermore, regression analysis on observations is done at 1_x1_ resolution (lines 207-208) while for model outputs the regression analysis is done at 2_x2.5_ resolution. But at what resolution are the reconstructed projections done? at the observation or the model resolution? Potential impacts on the regression coefficients due to different resolution should also briefly be discussed.

For future projection, the regression coefficient is interpolated to a 2° by 2.5° grid to be consistent with model output. So the projected DOD is also on a 2° by 2.5° grid. We modified lines 282-284 to clarify this and discuss potential impacts of the interpolation: “The regression coefficients are interpolated from the 1° by 1° grid to a 2° by 2.5° grid to be consistent with model output. Such an interpolation may smooth out some spatial characteristics from observations.”

4. I find it confusing that the paper is build around the seven CMIP5 models with interactive dust emissions to examine their performance to simulate DOD. But when presenting and describing the projections, the reconstructed ones based on the 16 models are considered. I understand and agree with the authors in the reasons to include more models, but then I would have expected that when examining the model performance (both climatology and interannual variability) these reconstruction (from the 16 models) also would be considered in order to be able to draw any conclusion from their projections. How good do these reconstructed projections (16 models) perform when compared with observations in present conditions? Sure, outputs of figure 9 and S8 are similar, but are they for the same reasons? Unfortunately analysis in figure 6 cannot be reproduced for the 16 models. Maybe it would make more sense to base results with respect to reconstructed projections in section 3.3 on figure S8 and move current figure 9 to the supplement (basically swaoing as it is now) and then build on how these results

are also seen (or not) in the 16 models.

We use seven CMIP5 model with interactive dust emission scheme because we would like to examine the relationship between DOD variations and local controlling factors, while in models with offline dust these connections are lost. We added lines 210-212 to better explain this. The purpose of using variables from 16 CMIP5 models for the future projection is to include as much information (i.e., more model output) about projected change of the controlling factors as possible.

We agree with the reviewer that it is better to show the future projection by the regression model and output from seven CMIP5 models in Figure 9 first and then discuss results from 16-model output later in Figure S7 in the Supplement. We followed the advice to switch the figures and modified text accordingly (lines 522-527, 549-557).

Here we also examine the climatology and interannual variations of reconstructed DOD (using 7-model output). The following figure shows the pattern correlation between MODIS DOD and reconstructed DOD using 7-model output and regression coefficients from observations. Figure R1a shows the pattern correlations between the climatologist of reconstructed DOD (regDOD) and MODIS DOD for 2004-2016 over 9 regions. The pattern correlations are very high, because the constant value in the regression model (i.e., d in the equation $regDOD = a \times Precipitation + b \times Wind + c \times Bareness + d$) contains information from MODIS DOD, i.e., has a pattern similar to observed climatology.

We also show the anomalies of the reconstructed DOD where the influence of the constant value is largely removed. Figs. R1b-c show pattern correlations between MODIS DOD and regDOD for the differences of DOD between 2010-2016 and 1861-2005 (Fig. R1b) and between 2010-2016 and 2004-2016 (Fig. R1c). The latter (Fig. R1c) shows slightly better pattern correlations than the former (less green boxes) since the historical condition (1861-2005) is not exactly comparable with the 2004-2016 climatology. Fig. R1d shows the pattern correlation of MODIS and regDOD for the differences of DOD between 2010-2016 and 2004-2009. The pattern correlations are similar to Fig. R1c because relatively short time periods are used (7 years for the 2010-2016 mean and 6 years for the 2004-2009 mean) and values can be largely influenced by interannual variations of the controlling factors in the CMIP5 models.

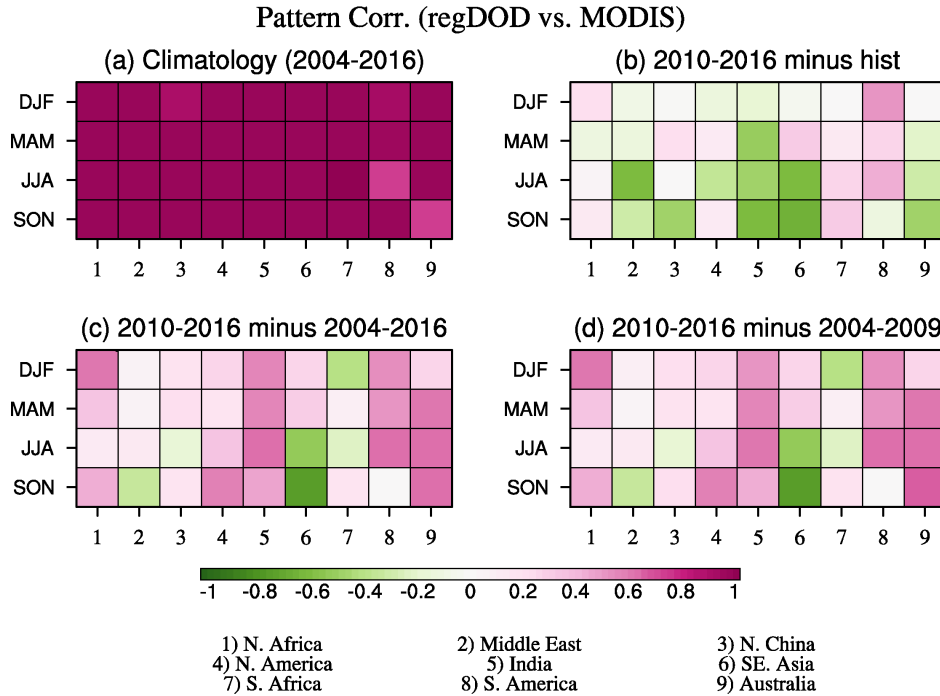


Figure R1. Pattern correlations between MODIS DOD and reconstructed DOD (regDOD) that used output from seven CMIP5 models and observed regression coefficients for (a) 2004-2016 DOD climatology, the differences of DOD (b) between 2010-2016 and historical run, (c) between 2010-2016 and 2004-2016, (d) between 2010-2016 and 2004-2009 over nine regions. MODIS DOD anomaly during 2010-2016 (with reference to the 2004-2016 climatology) is used in calculating pattern correlations in both (b) and (c).

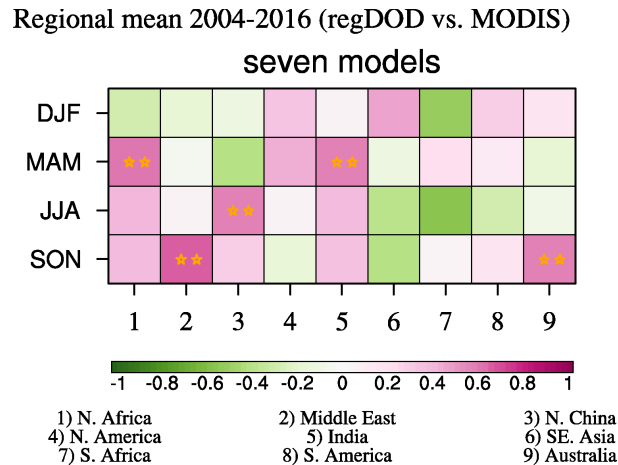


Figure R2. Correlations of regional averaged time series over nine regions between MODIS DOD and reconstructed DOD that used output from seven CMIP5 models and observed regression coefficients. Correlations significant at the 90% confidence level are marked by a star and significance at the 95% confidence level by two stars.

The correlations of regional averaged time series (2004-2016) between MODIS DOD and reconstructed DOD that used 7-model output and regression coefficients from observations are shown in Figure R2. As we mentioned in the paper, CMIP5 models are not expected to capture the interannual variations of the controlling factors, so we would not expect that the reconstructed DOD using CMIP5 output to capture the interannual variations of DOD, either. However, the variations of DOD over Africa in MAM, the Middle East in SON, India in MAM, and Australia in SON are to some extent captured by the regression model (Fig. R2). When we use observed controlling factors to reconstruct DOD (section 2.4.2), interannual variations during the present day is largely captured (Table S1).

The outputs of old Figs. 9 (from 16 models) and S8 (from 7 models) are similar because the projected changes of precipitation, surface wind speed, and bareness from 16-model ensemble mean (Fig. R3) show some features similar to 7-model ensemble mean (Fig. 8). We clarified this in the updated text (lines 549-557) and also added Fig. R3 to the supplement.

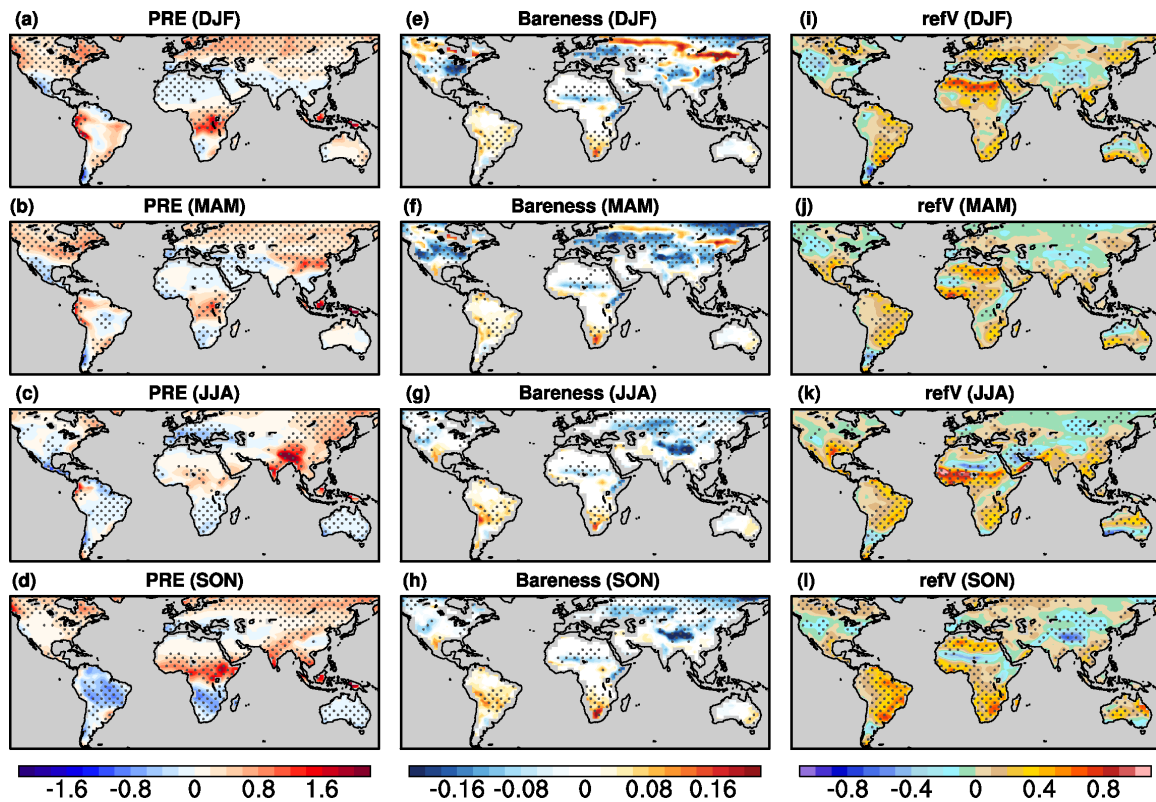


Figure R3. Projected difference of (a)-(d) precipitation (mm day^{-1}), (e)-(h) bareness, and (i)-(l) 10 m wind (m s^{-1}) between the late half of the 21st century (2051-2100; RCP 8.5 scenario) and historical level (1861-2005) from multi-model mean of 16 CMIP5 models. Areas with sign agreement among the models reaches 62.5% (i.e., at least ten out of 16 models have the same sign as the multi-model mean) are dotted.

Specific Comments:

Page 5, lines 73-75: See general comment above, I would suggest reformulating the statement.

We modified those lines to: “A comprehensive evaluation of the climatology and interannual variation of global dust optical depth (DOD) in CMIP5 models will provide insights into models’ capability of simulating the integrated aerosol extinction due to dust. DOD is also one of the key variables that determine radiative forcing of dust to the climate system.”. And also added discussion in lines 604-609 to acknowledge that DOD does not reflect the vertical distribution of dust aerosols and more variables (such as surface dust concentration, emission, deposition, vertical distributions) are needed to provide a whole picture of dust simulation in CMIP5 models.

Page 6, lines 98-100: Given the importance of DOD in this study I suggest you briefly describe the method how DOD was derived from AOD and specify the modifications you applied to adapt the method to collection 6.

Lines 102-114 are added to describe how DOD is derived and adapted to collection 6.

Page 7, line 134: Table 2 is referenced without any reference to Table 1. At present Table 1 corresponds to information on the models used in this study which is addressed in section 2.3. Tables should be arranged according to the order they are referenced in the text.

We actually referred Table 1 in line 78 when introducing the seven models used in this study.

Page 8, lines 138-143: Surface wind speed, bareness and precipitation are defined as controlling factors without providing any evidence or explanation why these parameters. However in lines 321-331 the authors explain why these parameters have been selected. I suggest moving these lines forward to section 2.2.

We follow the advice to move lines 321-331 to section 2.2 (now lines 167-176).

Page 8, line 156: Remove PRECL.

Here we refer to the precipitation data from PRECL and so will keep “PRECL precipitation”.

Page 9, lines 164-182: A reference to (current) Table 1 should be made in this section. In addition, information on the 16 models used in the future projections needs to be provided.

We added “Table 1” in line 207. We also modified lines 286-288 to clarify that information on 16 CMIP5 models can be found from the Supplementary Table S1 of Pu and Ginoux (2017).

Page 10, line 188: Provide a reference for the mass extinction efficiency used.

The mass extinction efficiency used here is from Ginoux et al. (2012a) as mentioned in line 231. We also added discussion on this variable in lines 237-241.

Page 10, lines 191-201: The authors illustrate the difference between the derived DOD and simulated one from one of the seven CMIP5 models with interactive dust emissions. It seems arbitrary why this model is used and not any other of the seven models? Is the intention of these lines to validate the derived DOD and therefore the chosen method? If that's the case then a more thorough validation should be done such as comparing the derived model mean DOD from all 16 models to the model mean from the seven CMIP5 models. Otherwise I don't see the point of having these analysis.

In these lines we compare the derived DOD versus model calculated DOD in GFDL-CM3 to valid the method we used to derive DOD (i.e., Eq. e). We did not use this analysis to select models. We chose seven models with interactive dust emission schemes to examine DOD climatology and interannual variations because DOD in these models are influenced by environmental factors and the can be compared with observations, while in models with offline dust, these connections do not exist in the models.

We used GFDL-CM3 as an example to validate the DOD derivation because it's the only model among the seven that we can access model calculated DOD. We modified lines 241-253 to better present the analysis.

Page 11, lines 216-220: What period is considered in this analysis, same as observations, ie 2004-2016?

Yes. We modified line 271 to clarify this.

Page 11, line 226: Please provide some information on these 16 models, which models are they? Are the seven model with interactive dust emission part of these 16 models? Do they have prescribed emissions? A similar table as Table 1 should be included with relevant information of these 16 models.

Seven models are part of these 16 models. We modified line 286-288 to clarify that models information and dust emission schemes can be found from Supplementary Table S1 of Pu and Ginoux (2017).

Page 13, lines 258-260: How do the authors explain the shift to the north in the DOD by HadGEM2?

In lines 258-260 (original version) we referred the multi-model mean shown in Fig. 2b: “The peak around 19° N in North Africa and Middle East is well captured by the multi-model mean, although the magnitude is slightly underestimated.” The overestimation of DOD around 28° N in the HadGeM2 model may be caused by its overestimation of DOD over the Middle East and India in summer (Figs. 3b, e).

Page 13, line 269: remove “than other seasons”.

Done.

Page 13, line 270: add “by the model mean” after “captured”.

Done.

Page 13, lines 269-271: Since individual models are illustrated, authors should not only focus on the multi model mean but also on the individual models and their differences with respect to the multi model mean and the observations. For instance, MIROC and

GFDL do not present the observed variability, in particular over N. America and India and they also present a different variability than the other models over northern China, with the peak closer to the observed one.

We revised lines 334-337, 345-347, 358-359 to add discussion on a few models' performance over North America, northern China, and Australia.

Page 14, lines 276-277: The MODIS DOD peak in Australia is hardly seen.

We have scaled MODIS DOD over Australia ten times in Fig. 3 and modified figure caption accordingly to better display the seasonal cycle of DOD.

Page 15-16, lines 319-321: Which reconstructed DOD is used here? is it the one considering observed regression coefficients and simulated controlling factors? Or is it the one using simulated regression coefficients derived from model DOD and model controlling factors? Also, are only the seven CMIP5 models with interactive dust emission considered? The authors should be more specific which reconstruction they refer. Also, couldn't the correlation based on reconstructed DOD be integrated in the figure as an additional column?

The reconstructed DOD used observed regression coefficients and observed controlling factors. We modified lines 398, 412-414 to clarify this. We actually considered adding a column to Fig. 5 to show the correlations between MODIS DOD and reconstructed DOD (see Fig. R4 below) in the early version of the paper. However, since the reconstructed DOD here used observed controlling factors, which make it slightly "unfair" to compare the results with those from CMIP5 DOD, we decide to present the results separately in Table 2.

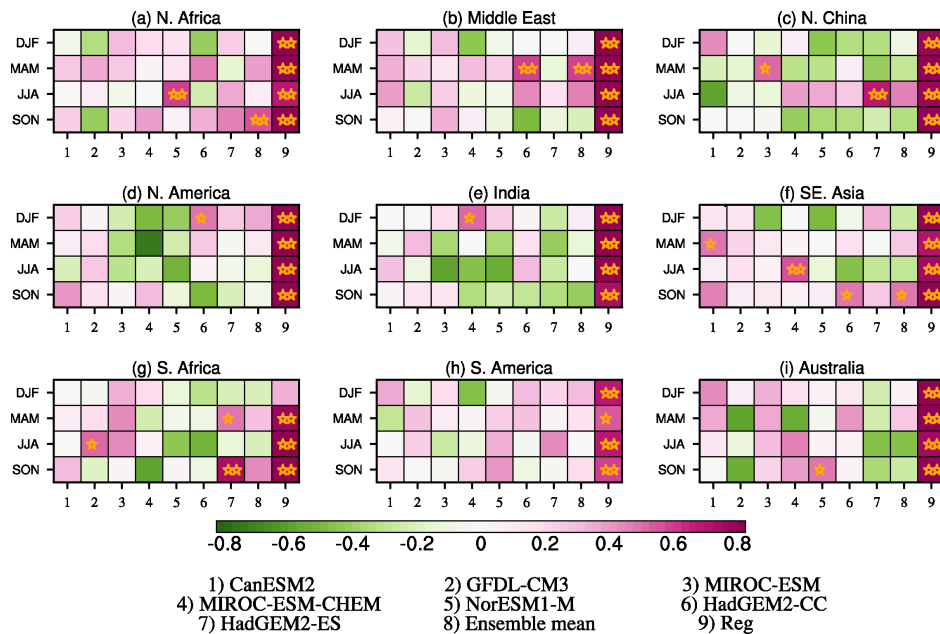


Figure R4. Correlations (color) between regional averaged time series from CMIP5 DOD and MODIS DOD from 2004 to 2016 for four seasons. Numbers in the X-axis denotes each model (1-7), multi-model mean (8), reconstructed DOD (9). Correlations significant

at the 90% confidence level are marked by a star and significance at the 95% confidence level by two stars.

Page 16, lines 321-332: move these lines to section 2. See general comment.

Done.

Page 18, lines 378-380: I have difficulties seeing the similarities in North Africa and the Middle east between the MODIS and CMIP5 regression coefficients pointed out by the authors. I actually see more the differences between both regressions in both regions. I would suggest the authors review the analysis in these lines.

Lines 458-462 are modified clarity this: “In JJA, the influences of precipitation and bareness over the eastern Arabian Peninsula in the multi-model mean (Fig. 6g) also show some similarity to observation (Fig. 6c), although an underestimation of the influence from bareness and an overestimation of precipitation are still there. “

Page 22, lines 470-473: On which results are the authors basing this statement. I suggest specifying.

We added “in the present-day (Fig. 6)” after “Multi-model mean also overestimates the connection between DOD and precipitation and surface wind and underestimates the influence of bareness” to specify this argument. In section 3.2 we compared the multiple linear regression coefficients from CMIP5 models with those from the observations (Fig. 6) and found multi-model mean overestimates the connection between DOD and precipitation and surface wind while underestimates the influence of bareness.

Pages 22-23, lines 465-490: These lines would fit better in the discussion section.

We prefer to discuss the uncertainties of CMIP5 and regression model projections right after showing the results of the two methods (Figs. 7-10) in section 3.3. In section 4, more general issues such as including other variables from CMIP5 models to examine model performance, studies on future dust projection, and the implication of the regression model, are discussed.

Page 24, line 522-524: The statement seems something that would fit better in the conclusion section. Consider moving it.

This is not the key conclusion of the paper, so we prefer to keep it in the discussion.

Page 25, line 546: Suggest replacing “quite well” with something more academic.

We modified the line to: “In JJA, the simulated zonal mean DOD from multi-model mean largely resembles MODIS DOD”.

Page 27, line 583: In which way are similarities between both projections “informative”? What information do they provide.

See our detailed reply to Comment #2. We removed “which may be informative”, and modified the sentence to: “we find some similarities between the two, which adds to the confidence of projected DOD change in these regions, for instance...”

Interactive comment on “How reliable are CMIP5 models in simulating dust optical depth?” by Bing Pu and Paul Ginoux
Anonymous Referee #2

We thank the reviewer for very helpful comments. We reply to your comment (in *Italic*) below.

The article presents an in-depth analysis of the CMIP5 models ability to reproduce the dust optical depth (DOD), considering both seasonal and inter-annual variability, as well as the driving factors behind those DOD levels. The observational data used are DOD over land derived from MODIS Terra-aqua data; bareness derived from AVHRR; 10m wind speed from ERA-Interim reanalysis; and precipitation from PRECL. The analysis of the driving factors is performed by regressing the observed DOD from MODIS over land to the observed/reanalyzed driving factors. The analysis is then extended to future climate scenarios (RCP8.5) using both the CMIP5 models’ dust outputs and the regression based on present day observed relationships between DOD and the driving factors.

The main results/conclusions are: 1) Models behave better over the NH large dust sources. 2) Models do not reproduce interannual variability. 3) The constraints from bareness in models are underestimated and the influences of wind speed and precipitation are overestimated. 4) A corrected projection of DOD based on the regression model is proposed. There are some similarities between the projections and the corrected projections.

The paper is very interesting, includes novelties and deserves publication. However, I have several doubts and comments that need clarification and further discussion.

General comments

1) DOD from MODIS: It is not clear what the DOD derived from MODIS refers to. Is it total dust optical depth or coarse dust optical depth? I understand that it refers to the total dust optical depth (fine and coarse) but I was confused when the product was compared to the coarse (O’Neill) product from AERONET. Can you please explain better the derivation of DOD from AOD in the paper? Given the importance of the dataset for the paper I feel it is not enough to refer the reader to other publications. Also, can you provide an estimation of the uncertainty of this product?

We added lines 102-114 to better explain how DOD is derived. It is coarse dust optical depth. The formula is derived from the work of Anderson et al. (2005). Uncertainty of this product is added to the supplementary information as shown below. We also modified lines 119-122 to include these information.

Figures R1-2 compares aerosol optical depth (AOD) between MODIS and AEROSOL ROBOTIC NETWORK (AERONET) sites data (top), and between MODIS DOD and AERONET coarse mode aerosol optical depth (COD; bottom). AERONET COD is processed by the Spectral Deconvolution Algorithm (O’Neill et al., 2003). We used an evaluation method following Levy et al. (2003; their Fig. 11) for AOD and COD errors. The AERONET Level 2 (quality assured) 10 minutes AOD and COD (500 nm) are extracted for Aqua equatorial crossing time (1:30 PM) and Terra equatorial crossing time (10:30 AM) plus or minus 30 minutes, and are considered if there is at least 2

measurements per day and there should be at least 100 days with data. We select AERONET sites within a spatial radius of 15 km of MODIS measurement. 883 AERONET sites are used. Total number of valid data is about 35,747. In box-whisker plots (e.g., Fig. R1), all collocated MODIS and AERONET data are grouped into bins of 500 measurements. The last bin will contain a larger number of values corresponding to the remaining of the division.

As shown in Fig. R1, MODIS slightly underestimated Aqua AOD and DOD for most of the AOD and DOD ranges. Compared to AERONET station data, Aqua AOD is underestimated, and DOD largely inherits this error. For Aqua DOD around 0.50, the median error is around 0.08, with estimated errors ranging from -0.29 to 0.16. Terra DOD is better than Aqua DOD in terms of the median of errors (Fig. R2 bottom vs. Fig R1 bottom). The median error for Terra DOD around 0.50 is very close to zero, with estimated errors ranging from -0.23 to 0.25.

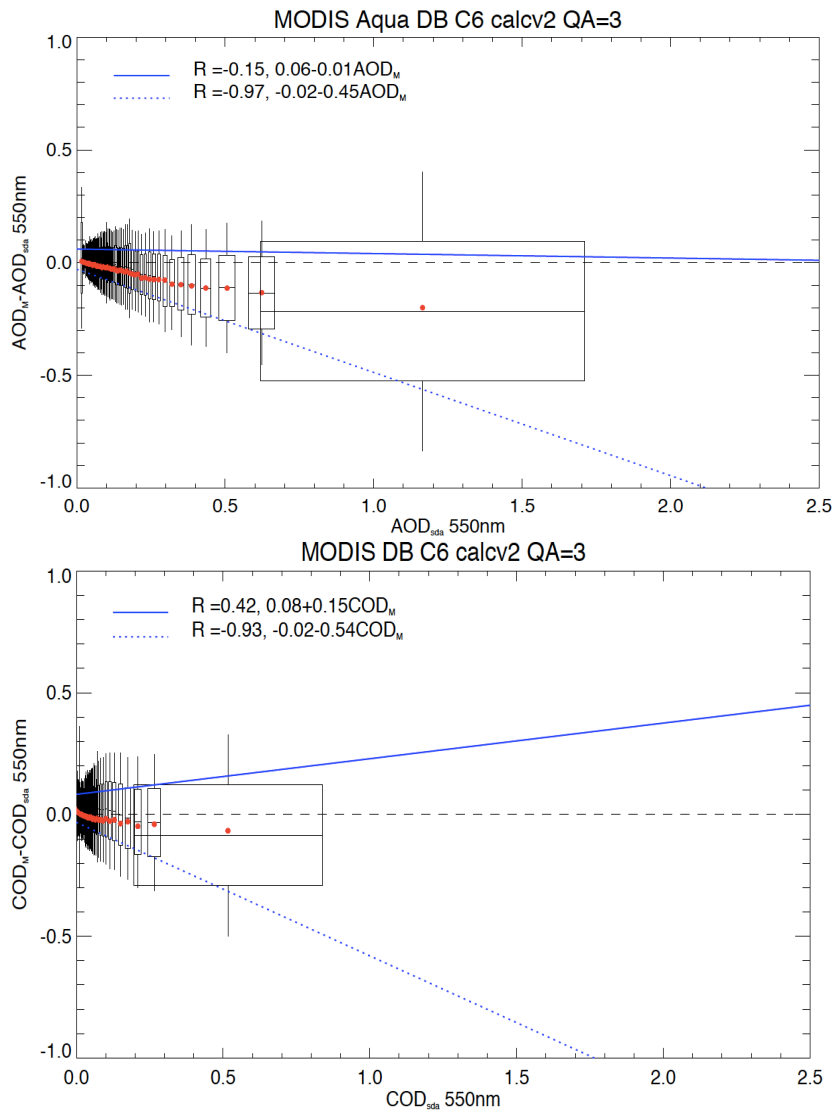


Figure R1. Comparison between grouped Aqua AOD error (i.e., the differences between MODIS AOD and AERONET AOD versus AERONET AOD, top), and grouped coarse mode aerosol optical depth (COD) error (i.e., the differences between MODIS DOD and AERONET COD versus AERONET COD, bottom). For each box-whisker, its width is 1σ of the AOD (COD) bin, while its height, whiskers, middle line and red dots are the 1σ , 2σ , mean, and median of AOD (COD) error, respectively. The envelope of estimated errors are blue and the one-one line (zero error) is dashed black.

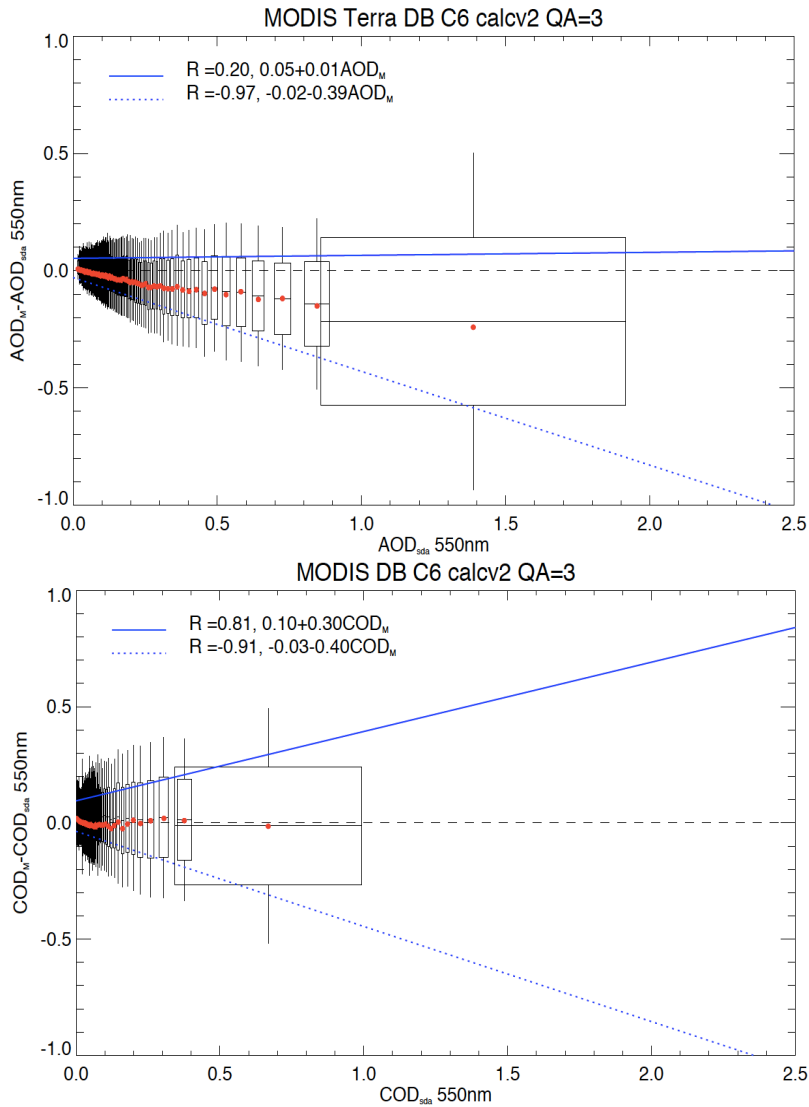


Figure R2. Same as Fig. R1 but for Terra DOD.

The confidence of satellite data over the different regions is assessed by comparison with AERONET (few stations, low spatial coverage), CALIOP, and considering the number of days with available DOD per season. Results show that while in Africa, South America, Middle East and some Asian regions confidence seems to be high, for some regions in

Asia/North America it largely depends on the season. In my view, the strength or confidence on the DOD data by region should be considered when discussing: the modelled DOD evaluation at the regional level, the regression method projections and discrepancies with CMIP5 models.

Major uncertainties we found in terms of days of coverage and comparison with AERONET and CALIOP are: 1) low coverage over northern China and Southeastern Asia in JJA; 2) DOD is slightly higher than COD from AERONET over Arabian Peninsula in DJF and SON; 3) DOD is lower than CALIOP COD over northern India in MAM. We added lines 159-164, 338-343 to discuss the uncertainties associated with DOD.

2) DOD from CMIP5 models: The authors compare the DOD derived from the selected CMIP5 models using Eq. (2). Using a value of 0.6 everywhere and for every model is an important simplification as it depends on model-dependent assumptions on size distribution and other issues such as the size range considered. While 0.6 may be a reasonable value for GFDL-CM3, how can we be sure it is ok for other models? Is there any other model for which you could compare this assumption in addition to GFDL-CM3.

We agree that using 0.6 for all models is a simplification and adds uncertainties to our analysis. We modified text to address this issue, e.g., added lines 237-241: “Applying the same mass extinction efficiency everywhere and to all the CMIP5 model output used here is a simplification, as different models may have quite different mass extinction efficiency. For instance, e can range from 0.25 to 1.28 $\text{m}^2 \text{g}^{-1}$ in AEROCOM models, with a multi-model medium of 0.72 $\text{m}^2 \text{g}^{-1}$ (Huneeus et al., 2011).” and lines 243-244: “A full validation of this method will require modeled DOD from all the other CMIP5 models, which are currently not available.”

3) Clear sky vs all sky values: While the authors have made an effort to gather the largest possible amount of DOD data by using both Aqua and Terra, the results of the comparison between MODIS DOD and model DOD may be quite affected by the use of all sky values from the models instead of clear sky values. Can you at least quantify this effect by for example using clear sky DOD from GFDL-CM3? How large is this effect? This may be potentially important in areas with seasonal clouds and precipitation. Could this be one of the reasons for the strong disagreement in some regions?

As the reviewer pointed out, MODIS AOD removed pixels contaminated by cloud, and therefore AOD (and DOD) is retrieved toward a clear-sky condition. On the other hand, the derived (or modeled) DOD in CMIP5 models does not have any cloud-screening process and therefore is under an all-sky condition. The inconsistency between the two may add some uncertainties in regions with more cloud coverage/amount, such as the central U.S., northern China, southeastern Asia, and northern South America, but less so over North Africa, South Africa, the middle East, Australia, India (except JJA), and Australia (Figure R3).

ISCCP Cloud Amount (1991-2012)

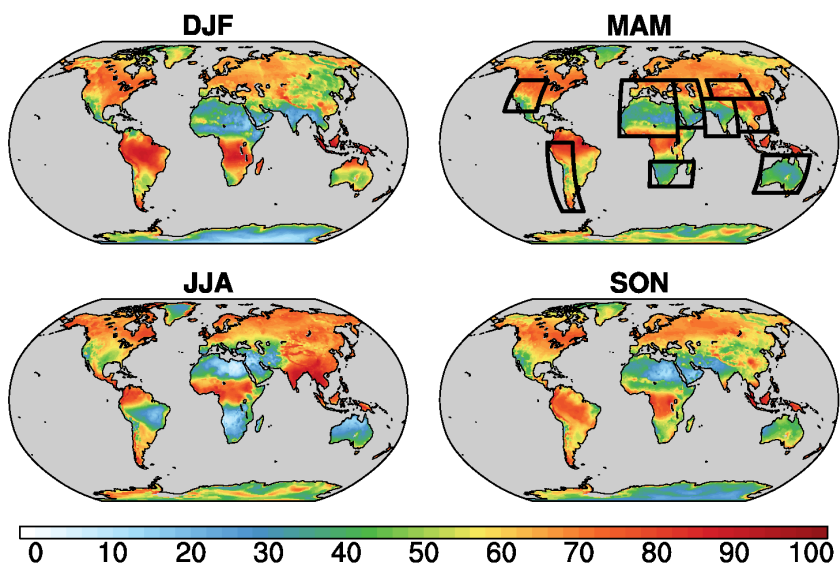
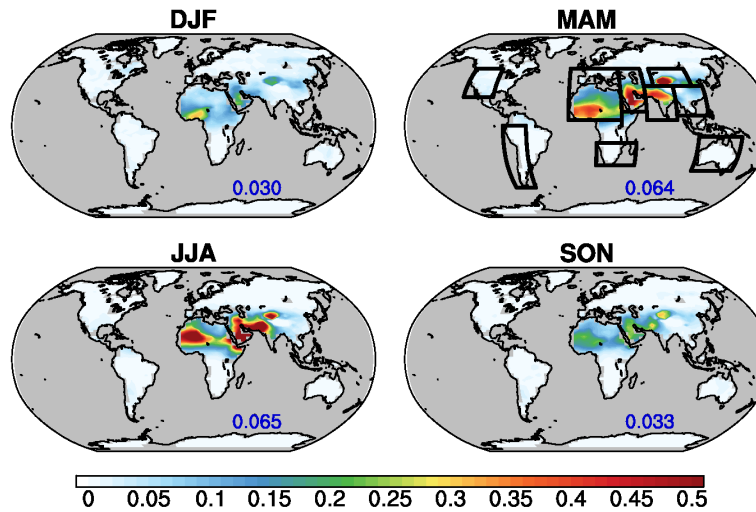


Figure R3. Total cloud amount (%) from the International Satellite Cloud Climatology Project (ISCCP) averaged over 1991-2012. Black boxes denote the nine averaging regions.

In GFDL-CM3 model, DOD at each grid point is calculated under all-sky condition and model does not have output of clear-sky DOD. We compared DOD from CALIOP level 3 data under all-sky condition and cloud-free (i.e., clear sky) condition (Figure R4). The differences of global mean DOD over land under all-sky and clear-sky conditions range from -0.003 in MAM to 0.001 in DJF. The differences are larger ($> \pm 0.05$) over cloudy regions in MAM and JJA, particularly over Guinea coast in West Africa, northern China, southeastern Asia, India (Fig. R4, bottom). The differences are largely due to the fact that much less samples are collected to produce cloud-free DOD over these cloudy regions (not shown). The disagreement between MODIS DOD and CMIP5 DOD in the above regions (i.e., Guinea coast in West Africa, northern China, southeastern Asia, India) is not particularly higher than other regions (e.g., Fig. 4).

CALIOP DOD 2007-2016 (all sky)



CALIOP DOD (all-sky minus cloud-free)

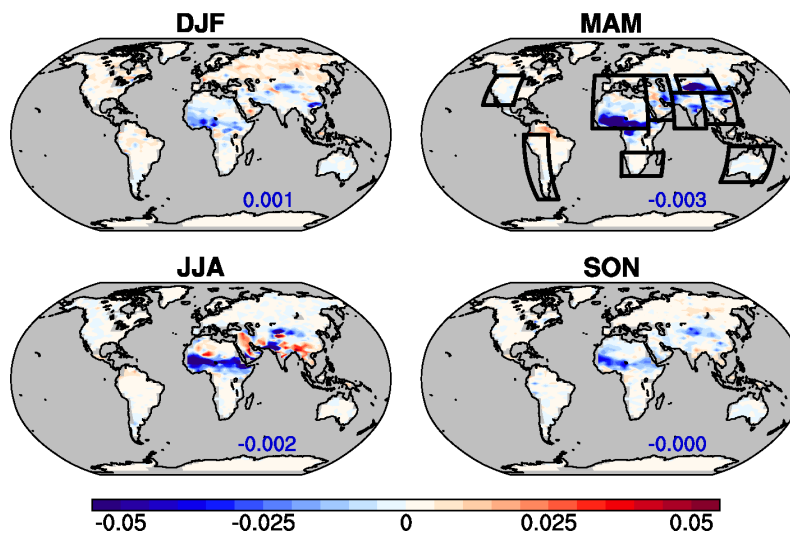


Figure R4. Climatology (2007-2016) of CALIOP DOD under all-sky condition (top) and the differences between all-sky and cloud-free conditions (bottom). Blue numbers denote global mean DOD over land.

4) *Interannual variability: One of the findings of this study is that the interannual DOD variation is not very well captured by the CMIP5 models. It is stated that “models probably misrepresented these [controlling factor] relationships, in addition to their incapacity of capturing the interannual variations of individual controlling factors”. Because of their nature, CMIP5 models cannot (and are not meant to) represent year-to-year variations of the driving factors in such a short time period. Therefore, the first part of the statement is just speculative, i.e., one cannot know whether the relationships are misrepresented from that analysis alone. I strongly believe that this part should be better discussed both in the results section and the conclusions. I also believe that the*

comparison between CMIP5 model output and observations in Figures S4 to S6 is not needed. Isn't it obvious that CMIP5 models cannot represent year-to-year variations of each season in a 12-year period?

The reviewer questioned our argument "...models probably misrepresented these relationships..." following the discussion on Figure 5 and Table S1. We did not intend to make any conclusion at that line, but to bring up a question. Later in Figure 6 we examined the connections between CMIP5 DOD and controlling factors. We revised line 425 to avoid misunderstanding: "... models may misrepresent these relationships, in addition to their incapacity of capturing the interannual variations of individual controlling factors in general". We also followed reviewer's suggestion to remove Figures S4-6 and modified text accordingly (line 427, lines 669-674).

5) The role of surface bareness: one of the important conclusions of the study is that "constraints from surface bareness are largely underestimated while the influences of surface wind and precipitations are overestimated". I have a few doubts/comments on this:

a. How can you know that the constraint from surface bareness is largely underestimated? Given your methodology, couldn't it be that the constraint of surface bareness is correct in absolute terms but the effect of precipitation (through soil humidity) is overestimated? This should be clarified.

It is possible that the magnitude of one controlling factor in the model is closer to the observation while the others are systematically underestimated/overestimated. So we standardized each controlling factor before regression. Therefore, the differences due to their absolute values are removed. The regression coefficients thus reflect how the interannual variations of each factor may contribute to the variations of DOD.

b. While I think that the methodology is sound, it is not clear to me how year-to-year variations of around 2-3 % in LAI (Figure S7) can have such an impact in the interannual variability of dust in Northern Africa. Because this conclusion has important implications, could you further discuss this point? What would be the physical mechanisms that could explain this?

First of all, we'd like to clarify that Fig. S7 shows bareness instead of LAI. Year-to-year variations of LAI are above 10% over the Sahel and parts of North Africa (Figure R5, right column). Bareness, or LAI, is a key non-erodible factor that can prevent wind erosion. The reason bareness shows a stronger influence on the interannual variations of DOD than the other two factors (precipitation and surface wind speed) is because its variations are more consistent with DOD changes. Here we show an example. We select an area over the Sahel (10°-16°N, 0°-25°E) where bareness is the dominant controlling factor in MAM based on multiple liner regression (Figure R6a). As shown in Figure R6b, the interannual variation of bareness (orange) is more consistent with DOD (black) variations than surface wind speed (green) or precipitation (purple) in the region. The correlation between DOD and standardized bareness is 0.61 (p=0.03), also higher than the correlations between DOD and precipitation (-0.46) or between DOD and surface wind (0.55).

We also examined multiple-linear regression using LAI from GLASS during 2004-2014 (Xiao et al. 2014). GLASS LAI is derived from MODIS products for years after 2001. The results using GLASS LAI are very similar to what we obtained from AVHRR LAI (Figure R7).

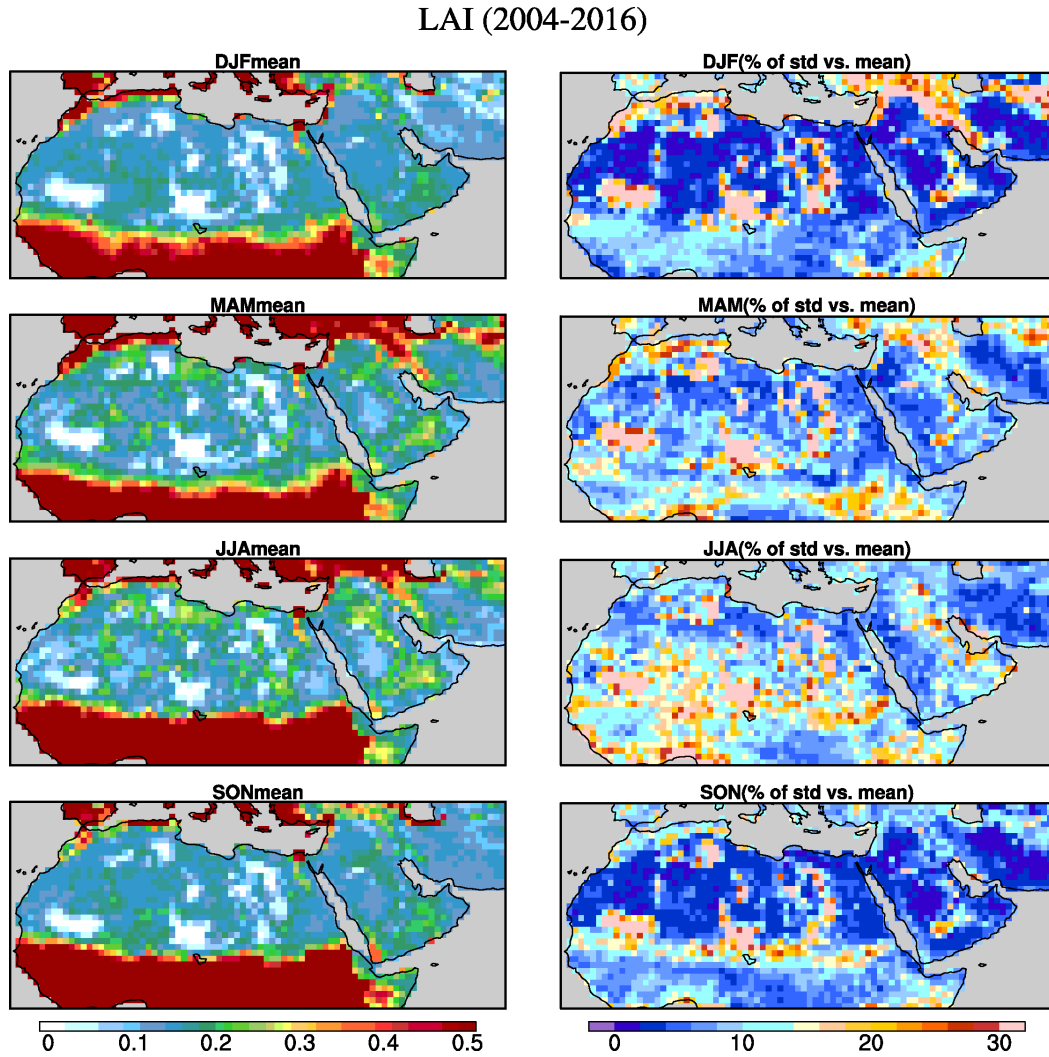


Figure R5. Seasonal mean of LAI averaged over 2004-2016 (m²/m²; left) and ratio (%) of standard deviation of LAI to seasonal mean LAI (right) over North Africa and the Arabian Peninsula from AVHRR during 2004-2016.

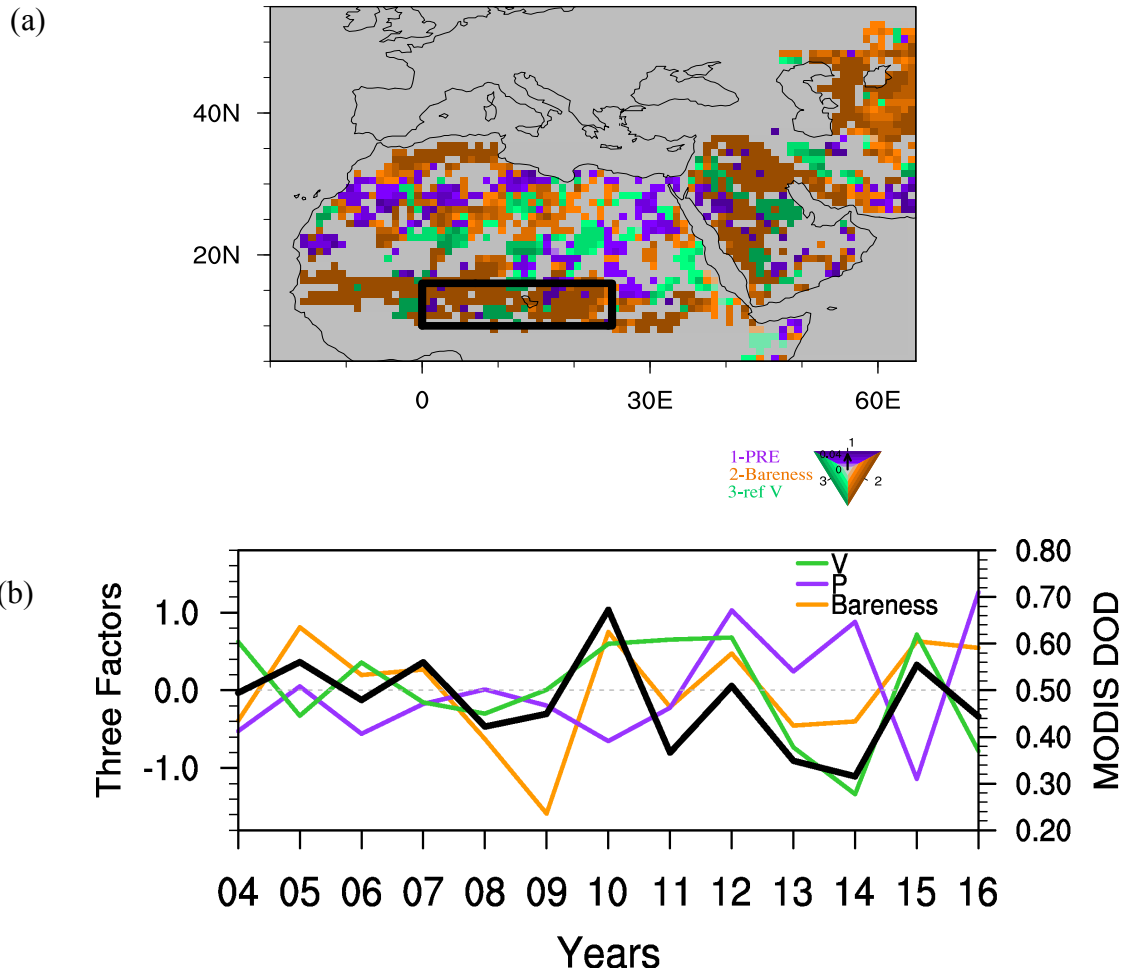


Figure R6. (a) Same as Fig. 6b but on a 1° by 1° grid for North Africa and the Middle East. Black box indicate an averaging area between 10°-16°N and 0°-25°E. (b) Time series of standardized controlling factors of bareness (orange), surface wind (green), precipitation (purple) and MODIS DOD (black) averaged over the area shown in (a).

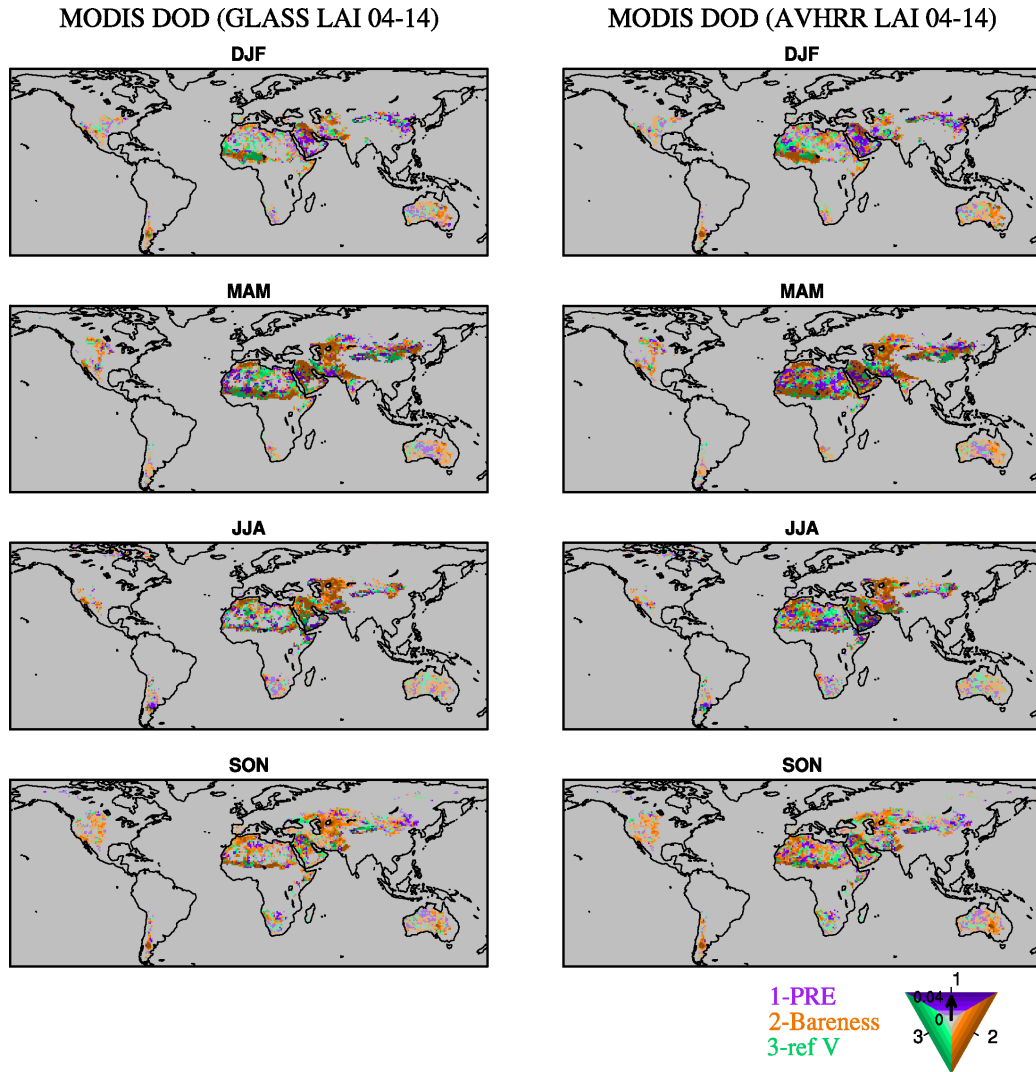


Figure R7. Regression coefficients calculated by regressing DOD in each season onto standardized precipitation (purple), bareness (orange), and surface wind speed (green) from 2004 to 2014. Coefficients obtained using MODIS DOD and observed controlling factors. Plots in the left used LAI from the GLASS, while on the right used LAI from the AVHRR. All the other variables are the same. The color of the shading denotes the largest coefficient in absolute value among the three, while the saturation of the color shows the magnitude of the coefficient (from 0 to 0.04). All regression coefficients regardless of their statistical significance are shown. Missing values are shaded in grey. To highlight coefficients near dust source regions, a mask of $LAI \leq 0.5$ is applied.

Can you provide the same figure (S7) but for the model derived bareness (both present day and future projections)? How well do the models compare with the observed range of variability of the LAI in arid regions (the Sahara for example)?

Modeled climatology of bareness is higher over North Africa (Figure R8) than that in the AVHRR, and the standard deviation is lower over northern North Africa but much higher over the Sahel.

Bareness (CMIP5) 2004-2016

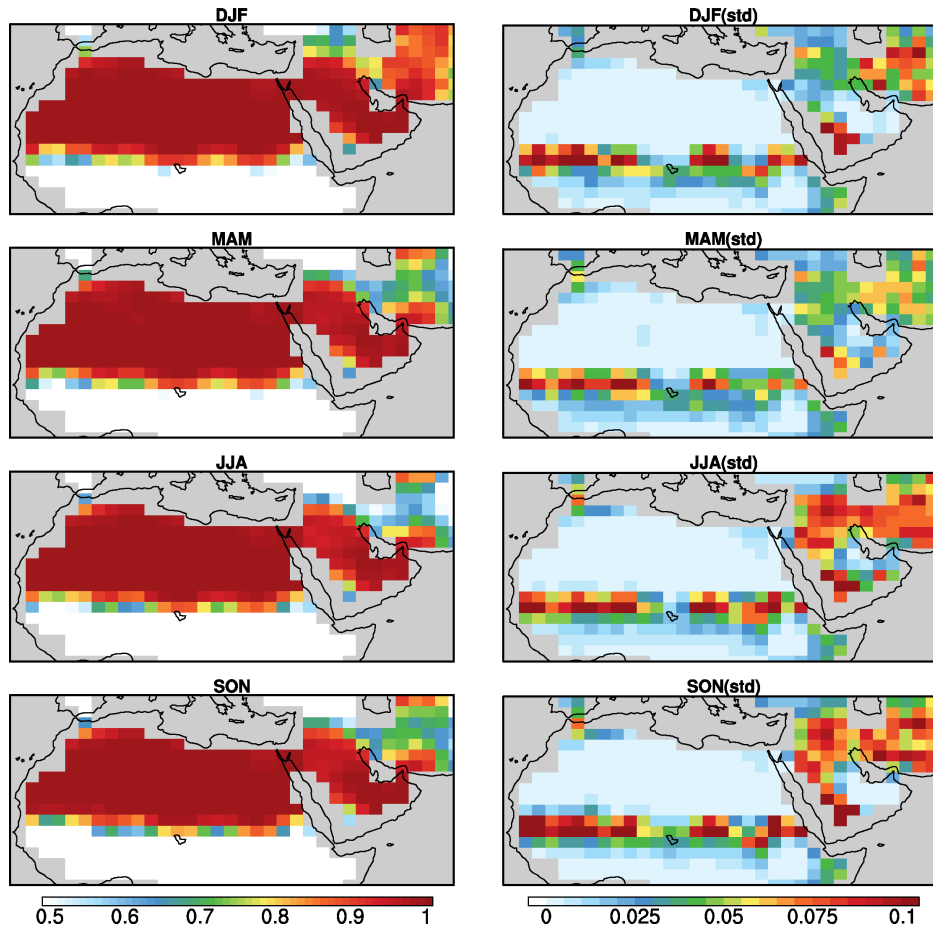


Figure R8. Seasonal mean (left) and standard deviation (right) of bareness over North Africa and the Arabian Peninsula from CMIP5 7-model ensemble mean during 2004-2016.

6) *Regression method projections vs. CMIP5 projections: The regression method used to derive DOD in future scenarios is based upon 16 CMIP5 model variables (surface wind speed, bareness and precipitation) and compared to dynamical projections of only 7 CMIP5 models (those with online dust schemes). Partly, differences in future trends might come by differences in driving variables. You state [line 439] that projected DOD changes using the full sample or only 7 models are very similar. If so, why not using the same 7 model outputs as drivers? This would enhance consistency. Finally, why the similarities between the two approaches in some regions may be informative?*

The purpose of using variables from 16 CMIP5 models for the future projection is to include as much information (i.e., more model output) about projected change of the controlling factors as possible. As the reviewer pointed that, different number of CMIP5 models used for the regression model may add to the differences between CMIP5 model projected DOD and regression model projected DOD. So we follow the suggestion to

show regression model projected DOD change using 7-model output in Figure 9 to keep the consistency and show results from 16-model in Figure S7.

We removed “which may be informative”, and modified the sentence to: “we find some similarities between the two, which adds to the confidence of projected DOD change in these regions, for instance...”. We also modified lines 513-522 to better explain approach of future projection using the regression model: “Here we also present the projected change of DOD from the regression model in Figure 9. The regression model is developed based on observed relationships between DOD and local controlling factors and can largely capture the interannual variations of DOD in the present-day climate (Table S1 in the Supplement). Assuming that the observed connection between DOD and these controlling factors do not change dramatically in the future, we can use this regression model and CMIP5-model projected change of controlling factors to project DOD variations. Compared to DOD projection from CMIP5 models, this approach utilizes additionally observational constrains and is likely to provide a more reliable future projection.” Although CMIP5 models overestimate the influence of surface wind and precipitation and underestimate the role of bareness, there are some similarities between model and observations (Fig. 6; lines 450-462), which indicate that models partially capture the connection between the DOD and these controlling factors in some regions. Therefore, the projection of DOD from CMIP5 models is not completely unreliable. The similarity between CMIP5 projection and the projection from the regression model thus adds to the confidence of projected change of DOD over North Africa, the Arabian Peninsula, and northern China in some seasons.

Minor comments:

- I suggest to list multiple references to the same topic chronologically, unless there are reason to order them differently, e.g. in the introduction.

Done.

- I think the column heading “Dust emission scheme” is somewhat misleading as the given references describe the implementation of a dust emission scheme, not the scheme itself. Perhaps rewording to “Dust emission implementation” or similar would help.

We follow the suggestion to change column head to “Dust emission implementation”.

- I suggest changing Eq. (1) to $Bareness = \exp(-LAI)$. Also, is there a reference for this equation?

We change Eq. (1) following the comment and added a reference.

- L. 146-147: I would normally not consider a resolution of 80km “very suitable to study the influence of wind speed on dust emission and transport on small scales”. I understand the intent of this statement, but I suggest rephrasing this to avoid misunderstanding.

Thanks for the suggestion. We modified lines 185 to “We choose this analysis because of its relatively high spatial resolution”.

- L. 160: I suggest to delete “relatively high” as well as “quite”
Done.

- L. 192: GFLD-CM3 should be GFDL-CM3
Done.

- Line 205: clarify which DOD is regressed onto observed values, i.e. satellite derived DOD

We changed the sentence to “by regressing MODIS DOD onto...”

- Fig. 3i: It is very hard to see the MODIS DOD pattern for Australia. Can this be improved?

We re-plotted the figure to better display MODIS DOD for Australia.

- Fig. 4 is ok, but quite dense

We updated the figure to make it look better.

- L. 311: variability instead of variations

Done.

- L. 328: wind erosion instead of “soil erosion from wind”

Done (now line 173).

- Line 431: centaury should be century

Done.

- L. 457 ff: Sometimes it is not clear if “models” refers to the CMIP5 models or projection ‘models’.

We changed “models” to “regression projections” to avoid confusion.

- Figure 6. It is difficult to sort out the different elements, e.g. the strength of the regression depending on the shading intensity is not visible. I would suggest: to make a zoom per region, or to display dependencies from the 3 variables in independent maps, and to use the same resolution for MODIS and CMIP5 maps to make easier a direct comparison.

We updated Figures 6 by interpolating results from MODIS and observed controlling factors to model grids (2° by 2.5° , Figs. 6a-d) and changed color scale from 0~0.02 to 0~0.04 to better show the shading intensity. We also zoomed in and plotted a few figures for different regions (Figures R9-R13) here. The patterns in new Fig. 6 are very similar to the old one. The connection between DOD and bareness is underestimated on the interannual time scale in CMIP5 models. On the other hand, DOD’s connection with precipitation and surface wind speed are overestimated.

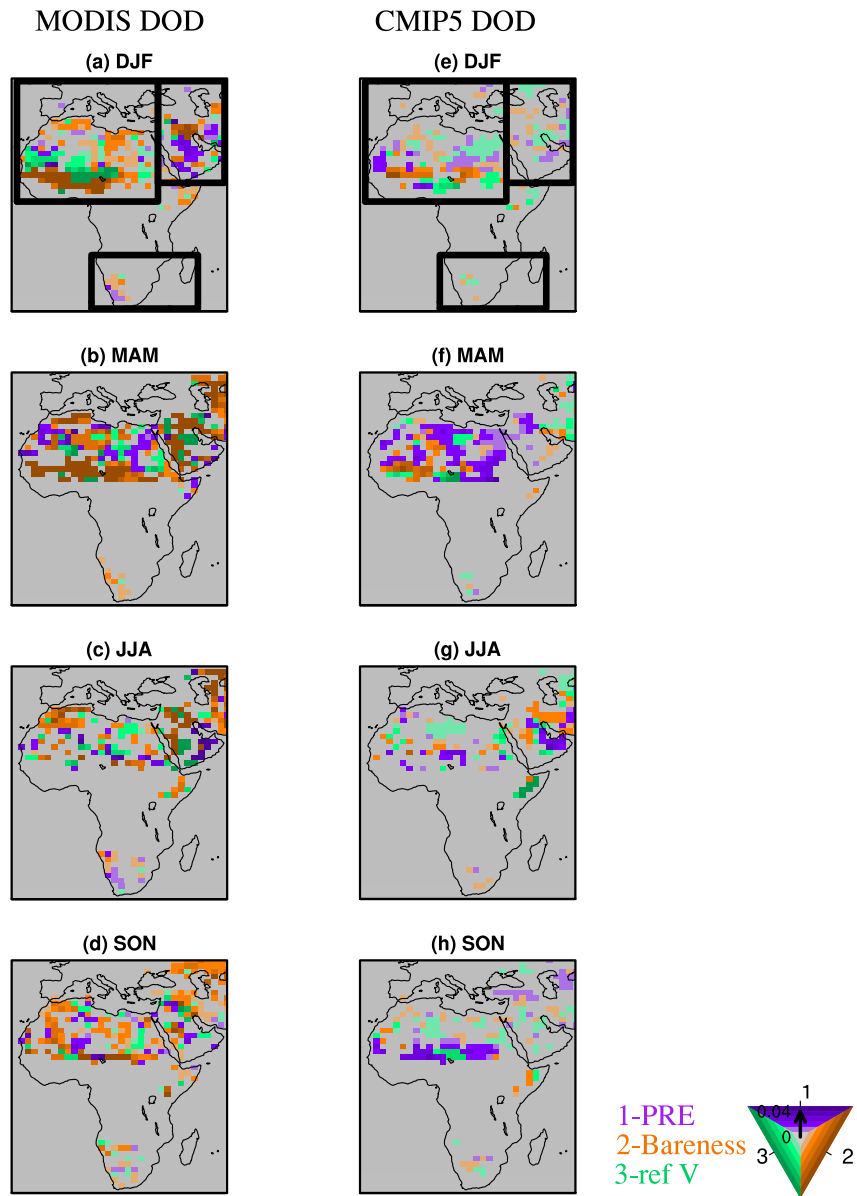


Figure R9. Same as Fig. 6 but for Africa and the Middle East. Black boxes denote the averaging regions defined in Table 2: North Africa, South Africa, and the Middle East.

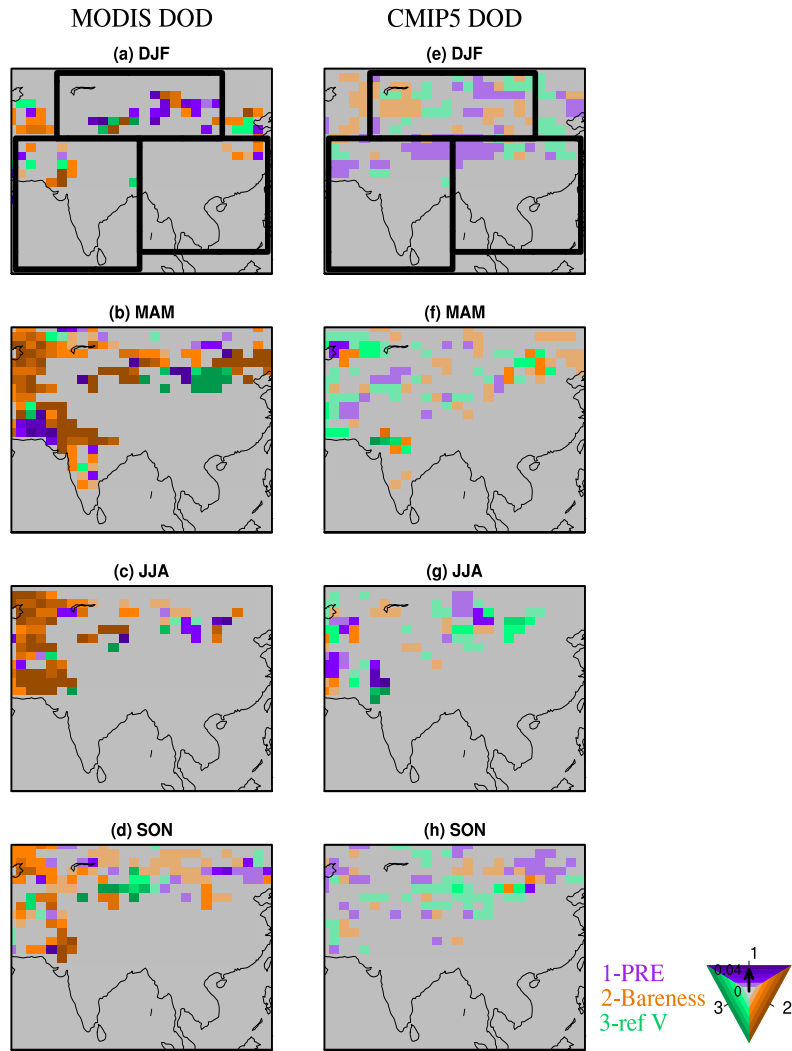


Figure R10. Same as Fig. 6 but for Asia. Black boxes denote the averaging regions defined in Table 2: northern China, India, and southeastern Asia.

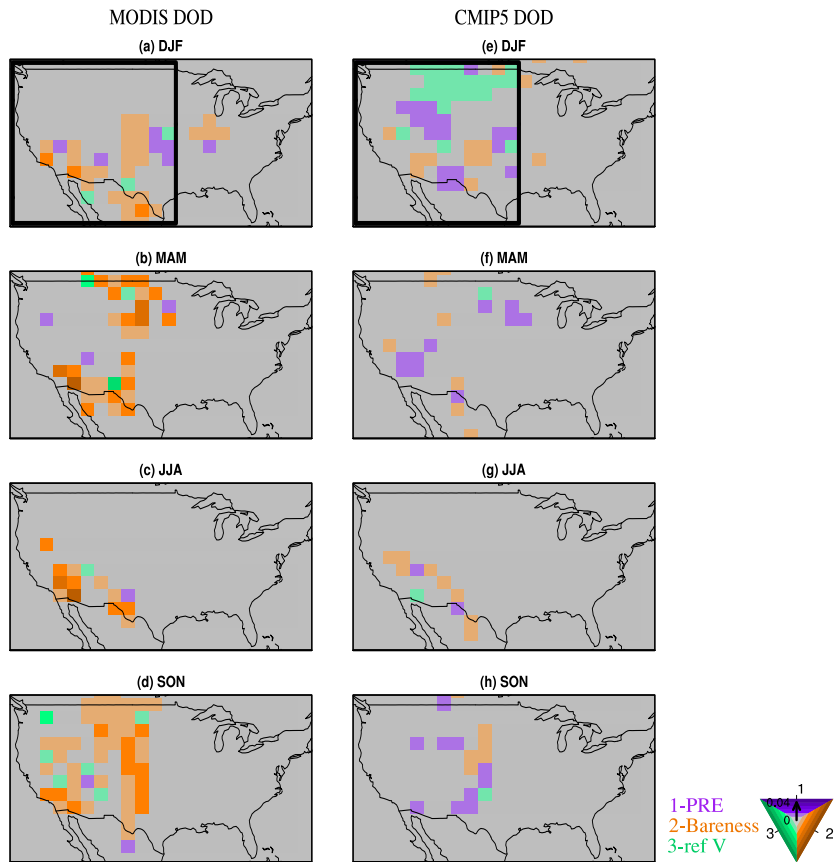


Figure R11. Same as Fig. 6 but for North America. Black boxes denote the averaging regions defined in Table 2: North America.

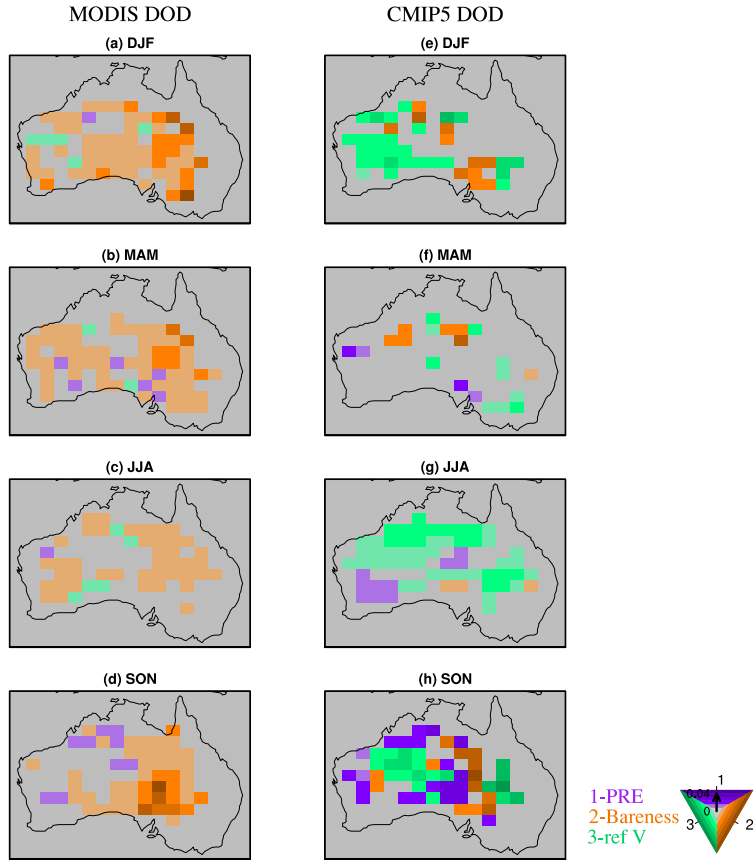


Figure R12. Same as Fig. 6 but for Australia.

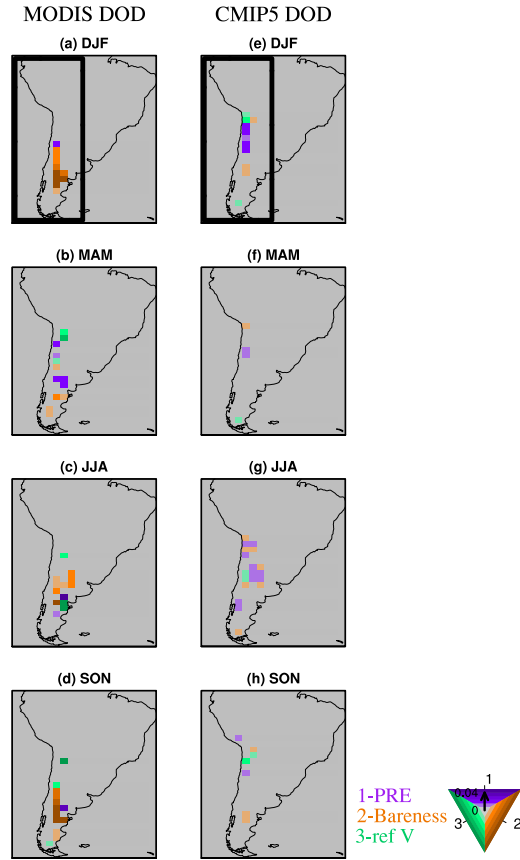


Figure R13. Same as Fig. 6 but for South America. Black boxes denote the averaging regions defined in Table 2: South America.

Reference:

Xiao ZQ, Liang SL, Wang JD, Chen P, Yin XJ, Zhang LQ, et al. Use of general regression neural networks for generating the GLASS leaf area index product from time-series MODIS surface reflectance. IEEE T. Geosci. Remote 52, 209-223 (2014)

How reliable are CMIP5 models in simulating dust optical depth?

Bing Pu^{1,2} and Paul Ginoux²

¹Atmospheric and Oceanic Sciences Program, Princeton University,

Princeton, New Jersey 08544

²NOAA Geophysical Fluid Dynamics Laboratory, Princeton, New Jersey 08540

Correspondence to: Bing Pu (bpu@princeton.edu)

1 **Abstract.** Dust aerosol plays an important role in the climate system by affecting the
2 radiative and energy balances. Biases in dust modeling may result in biases in simulating
3 global energy budget and regional climate. It is thus very important to understand how
4 well dust is simulated in the Coupled Model Intercomparison Project Phase 5 (CMIP5)
5 models. Here seven CMIP5 models using interactive dust emission schemes are
6 examined against satellite derived dust optical depth (DOD) during 2004-2016.

7 It is found that multi-model mean can largely capture the global spatial pattern
8 and zonal mean of DOD over land in present-day climatology in MAM and JJA. Global
9 mean land DOD is underestimated by -25.2% in MAM to -6.4% in DJF. While seasonal
10 cycle, magnitude, and spatial pattern are generally captured by multi-model mean over
11 major dust source regions such as North Africa and the Middle East, these variables are
12 not so well represented by most of the models in South Africa and Australia. Interannual
13 variations of DOD are neither captured by most of the models nor by multi-model mean.
14 Models also do not capture the observed connections between DOD and local controlling
15 factors such as surface wind speed, bareness, and precipitation. The constraints from
16 surface bareness are largely underestimated while the influences of surface wind and
17 precipitation are overestimated.

18 Projections of DOD change in the late half of the 21st century under the
19 Representative Concentration Pathways 8.5 scenario by multi-model mean is compared
20 with those projected by a regression model. Despite the uncertainties associated with both
21 projections, results show some similarities between the two, e.g., DOD pattern over
22 North Africa in DJF and JJA, an increase of DOD in the central Arabian Peninsula in all
23 seasons, and a decrease over northern China from MAM to SON.

24 1. Introduction

25 Dust is the second most abundant aerosols by mass in the atmosphere after sea
26 salt. It absorbs and scatters both shortwave and longwave radiation and thus modifies
27 local radiative budget and consequently vertical temperature profile, influencing global
28 and regional climate. For instance, studies found dust influences the strength of the West
29 African monsoon (e.g., Miller and Tegen, 1998; Miller et al., 2004; Mahowald et al.,
30 2010; Strong et al., 2015) and Indian monsoonal rainfall (e.g., Vinoj et al., 2014; Jin et
31 al., 2014, 2015, 2016; Solomon et al., 2015; Kim et al., 2016; Sharma and Miller, 2017).
32 Dust aerosols are also found to amplify droughts during the U.S. Dust Bowl and
33 Medieval Climate Anomaly (Cook et al., 2008, 2009, 2013), and affect Atlantic tropical
34 cyclones (e.g., Dunion and Velden, 2004; Wong and Dessler, 2005; Evan et al., 2006;
35 Sun et al., 2008; Strong et al., 2018). Dust particles can also serve as ice cloud nuclei and
36 influence the properties of the cloud (e.g., Levin et al., 1996; Rosenfield et al., 1997;
37 Wurzler et al., 2000; Nakajima et al., 2001; Bangert et al., 2012) and affect regional
38 radiative balance and hydrological cycle. When deposited in the oceans, iron-enriched
39 dust also provides nutrients for phytoplankton, affecting ocean productivity and therefore
40 carbon and nitrogen cycles and ocean albedo (e.g., Fung et al., 2000; Jickells et al., 2005;
41 Shao et al., 2011; ~~Jickells et al., 2005~~).

42 Globally, the estimated radiative forcing from dust aerosol is 0.10 (-0.30 to +0.10)
43 W m^{-2} , a magnitude about one fourth of the radiative forcing of sulfate aerosol or black
44 carbon from fossil fuel and biofuel (Myhre et al., 2013; their Table 8.4). Biases in dust
45 simulation may potentially affect global energy budgets and regional climate simulation.

46 Thus, it is very important to examine the capability of current state-of-the-art climate
47 models in simulating dust.

48 Only a few studies examined the Coupled Model Intercomparison Project Phase 5
49 (CMIP5) model output of dust and most of them are regional evaluations. For instance,
50 Evan et al. (2014) examined model output for Africa, but mainly focused on an area over
51 the northeastern Atlantic (10° – 20° N and 20° – 30° W) where a long-term proxy of dust
52 optical depth data over Cape Verde islands is available (Evan and Mukhopadhyay, 2010).
53 They found models underestimated dust emission and mass path and failed to capture the
54 interannual variations from 1960 to 2004, as models did not capture the negative
55 connection between dust mass path and precipitation over the Sahel.

56 Another work examined CMIP5 aerosol optical depth (AOD) is by Sanap et al.
57 (2014) for India. They compared dust distribution in the models with Earth Probe total
58 ozone monitoring system (EPTOMS)/ Ozone monitoring Instrument (OMI) aerosol index
59 (AI) from 2000 to 2005. They found most of CMIP5 models, except two HadGEM2
60 models, underestimated dust load over Indo-Gangetic Plains, and suggested the biases are
61 due to a misrepresentation of 850 hPa winds in the models. Later, Misra et al. (2016) also
62 examined CMIP5 modeled AOD for India but did not specifically focus on dust.

63 Shindell et al. (2013) examined the output of 10 models from the Atmospheric
64 Chemistry and Climate Model Intercomparison Project (ACCMIP) for one year (2000),
65 among which eight models also participated in the CMIP5. They noticed that simulated
66 dust AOD vary by more than a factor of two across models. However, this study also did
67 not focus on dust, but emphasized the radiative forcings from anthropogenic aerosols.

68 None of the above studies examined global dust simulation in CMIP5 models.
69 What's more, most studies focused on annual mean, not seasonal averages. It is very
70 possible that models perform better in some seasons than others. AeroCom multiple-dust
71 model intercomparison was performed on both global and regional scales (Huneus et al.,
72 2011) but only focused on one year, thus models' capability of simulating interannual or
73 long-term variability of dust is not clear. A comprehensive evaluation of the climatology
74 and interannual variation of global dust optical depth (DOD) in CMIP5 models will
75 provide ~~a clear picture of insights into~~ models' capability of ~~dust simulations~~ simulating the
76 integrated aerosol extinction due to dust, which is one of the key variables that determine
77 the radiative forcing of dust to the climate system.

78 Here we examine the results of seven CMIP5 models (Table 1) by comparing
79 model output with DOD derived from Moderate Resolution Imaging Spectroradiometer
80 (MODIS) Deep Blue aerosol products. Projections on changes of DOD in the late half of
81 the 21st century by CMIP5 models and also by a regression model (Pu and Ginoux, 2017)
82 are examined and analyzed.

83 The following section introduces data and methods used in this study. Results are
84 presented in section 3, including examinations on the climatology and interannual
85 variations of ~~modeled~~ CMIP5 DOD and future projections. Discussion and major
86 conclusions are presented in sections 4 and 5, respectively.

87

88 **2. Data and Methodology**

89 **2.1 DOD from MODIS**

90 DOD is a widely used variable that describes optical depth due to the extinction

91 by mineral particles. It is one of the key factors (single scattering albedo and asymmetry
92 factor being the two others) controlling dust interaction with radiation. Monthly DOD are
93 derived from MODIS aerosol products retrieved using the Deep Blue (MDB2) algorithm,
94 which employs radiance from the blue channels to detect aerosols globally over land even
95 over bright surfaces, such as desert (Hsu et al., 2004, 2006). Ginoux et al. (2012b) used
96 collection 5.1 level 2 aerosol products from MODIS aboard the Aqua satellite to derive
97 DOD. Here, both MODIS aerosol products (collection 6, level 2; Hsu et al., 2013) from
98 the Aqua and Terra platforms are used. Aerosol products such as AOD (550 nm), single
99 scattering albedo, and the Ångström exponent are first interpolated to a regular 0.1° by
100 0.1° grid using the algorithm described by Ginoux et al. (2010). The DOD is then derived
101 from AOD following the methods of Ginoux et al. (2012b) with adaptations for the newly
102 released MODIS collection 6 aerosol products (Pu and Ginoux, 2016). To separate dust
103 from other aerosols, we use the Ångström exponent (α) and single scattering albedo (ω).
104 Ångström exponent has been shown to be highly sensitive to particle size (Eck et al.,
105 1999). A continuous function relating the Ångström exponent to fine-mode aerosol
106 optical depth established by Anderson et al. (2005; their Eq. 5) based on ground-based
107 data is used to separate dust from fine particles. We also screen the data by setting single
108 scattering albedo at 470 nm to be less than one for dust due to its absorption of solar
109 radiation. This separates dust from scattering aerosols such as sea salt, which is purely
110 scattering. The formula can be summarized as the following:

$$111 \quad \underline{DOD = AOD \times (0.98 - 0.5089\alpha + 0.0512\alpha^2) \quad \text{if } (\omega < 1) \quad . \quad (1)}$$

112

113 Note that DOD represents the coarse mode fraction of dust only. It is estimated
114 that the fine mode dust at emission is less than 10% (Kok et al., 2017).

115 Aqua and Terra DOD have previously been used to study global dust sources
116 (Ginoux et al., 2012b), and their geomorphological signature (Baddock et al., 2016), dust
117 variations in the Middle East (Pu and Ginoux, 2016) and the U.S. (Pu and Ginoux, 2017),
118 and have been validated with Aerosol Robotic NETWORK (AERONET) stations over the
119 U.S. (Pu and Ginoux, 2017). Here we compare Aqua and Terra DOD against AERONET
120 stations globally (Section 1 and Figures. S1-2 in the Supplement). Both Aqua and Terra
121 DOD is slightly underestimated, with respective errors of $0.08+0.52DOD$ and
122 $0.10+0.48DOD$.

123 Daily DOD ~~is derived for both from~~ Aqua and Terra ~~satellites and then are~~
124 averaged to monthly data and interpolated to a 1° by 1° grid. Terra passes the Equator
125 from north to south around 10:30 local time while Aqua passes the Equator from south to
126 north around 13:30 local time. To reduce missing data and also to combine the
127 information from both morning and afternoon hours, a combined monthly DOD (here
128 after MODIS DOD) is derived by averaging Aqua and Terra DOD when both products
129 exist or using either Aqua or Terra DOD when only one product is available. As shown in
130 Figure S31 in the Supplement, the mean available days in each season and also spatial
131 coverage are enhanced in combined DOD than using Aqua or Terra (not shown) DOD
132 alone. This combined DOD is available from January 2003 to December 2016.

133 ~~Aqua and Terra DOD product has previously been used to study global dust~~
134 ~~sources (Ginoux et al., 2012b), dust variations in the Middle East (Pu and Ginoux, 2016)~~
135 ~~and the U.S. (Pu and Ginoux, 2017), and has been validated with Aerosol Robotic~~
136 ~~NETWORK (AERONET) stations over the U.S. (Pu and Ginoux, 2017). Here we~~

137 | We also compared MODIS DOD climatology with both AERONET observation
138 | and DOD retrieved from Cloud-Aerosol Lidar with Orthogonal Polarization (CALIOP;
139 | Winker et al., 2004; 2007) aboard the Cloud-Aerosol Lidar and Infrared Pathfinder
140 | Satellite Observation (CALIPSO) satellite. AERONET stations provide cloud-screened
141 | and quality assured (level 2) coarse mode aerosol optical depth (COD) at 500 nm, which
142 | is processed by the Spectral Deconvolution Algorithm (O'Neill et al., 2003). Only nine
143 | sites have long-term COD records during 2003-2016, and the climatological mean of
144 | MODIS DOD generally compares well with these sites (Figure S42 in the Supplement).

145 | CALIOP measures backscattered radiances attenuated by the presence of aerosols
146 | and clouds and retrieves corresponding microphysical and optical properties of aerosols.
147 | Monthly dust AOD (or DOD) on a 2° latitude by 5° longitude grid are available since
148 | June 2006. The climatology of CALIOP DOD during 2007-2016 is similar to that of
149 | MODIS DOD during the same period (Figure S53 in the Supplement). The global mean
150 | (over land) MODIS DOD is slightly higher than that from CALIOP, probably due to the
151 | lower horizontal resolution of the latter. The pattern correlations (e.g., Pu et al., 2016)
152 | between the two products range from 0.83 in boreal spring and summer to 0.63 in boreal
153 | winter (Figure S53 in the Supplement).

154 | Due to higher spatial resolution (compared with CALIOP) and coverage
155 | (compared with AERONET sites), MODIS DOD is chosen as the primary product to
156 | validate CMIP5 model output. Nine regions (Table 2) are selected to study the DOD
157 | magnitude, spatial pattern, and variations. These regions cover major dust source regions
158 | previously identified (Ginoux et al. 2012).

159 | Given the analysis above (Figs. S3-5), there are some uncertainties associated

160 with DOD in a few regions in some seasons: (1) relatively low coverage (<30 days per
161 season) over northern China and southeastern Asia in JJA; (2) DOD is slightly higher
162 than COD from AERONET over the Arabian Peninsula in DJF and SON; (3) DOD is
163 lower than CALIOP over northern India in MAM. We will consider these uncertainties in
164 the following analysis wherever is relevant.

166 **2.2 Reanalysis and observation datasets**

167 Previous study found that the variations of dust event frequency over the U.S. in
168 the recent decade could be largely represented by the variations of three local controlling
169 factors: seasonal mean surface wind speed, bareness, and precipitation (Pu and Ginoux,
170 2017). These factors have previously been found to constrain dust emission or variability
171 on multiple time scales (e.g., Gillette and Passi, 1988; Fecan et al., 1999; Zender and
172 Kwon, 2005). While surface wind is positively related to the emission and transport of
173 dust, vegetation is an important non-erodible element that prevents wind erosion.
174 Precipitation is generally negatively related to dust emission and transport processes.
175 While the scavenging effect of precipitation on small dust particles only lasts a few hours
176 or days, influences of precipitation on soil moisture lasts longer.

177 To examine the interannual variations of DOD and its connection with local
178 controlling factors such as surface wind speed, bareness, and precipitation, monthly data
179 of 10 m wind speed from the ERA-Interim (Dee et al., 2011), leaf area index (LAI) data
180 from Advanced Very High Resolution Radiometer (AVHRR; Claverie et al., 2014,
181 2016), and precipitation from the Precipitation Reconstruction over Land (PRECL; Chen
182 et al., 2002) are used.

183 ERA-Interim is a global reanalysis from the European Centre for Medium-Range
184 Weather Forecasts (ECMWF). Its horizontal resolution is T255 (about 0.75° or 80 km),
185 ~~We choose this analysis because of its relatively high spatial resolution very suitable to~~
186 ~~study the influence of wind speed on dust emission and transport on small scales.~~ The
187 monthly data are available from 1979 to present day.

188 Monthly LAI derived from the version 4 of Climate Data Record (CDR) of
189 AVHRR is used to calculate surface bareness. The data are produced by the National
190 Aeronautics and Space Administration (NASA) Goddard Space Flight Center (GSFC)
191 and the University of Maryland. Monthly gridded data on a horizontal resolution of 0.05°
192 by 0.05° degree are available from 1981 to present. This product is selected due to its
193 high spatial resolution and long temporal coverage. Surface bareness is calculated from
194 seasonal mean LAI (Pu and Ginoux, 2017) as the following,

$$195 \quad \text{Bareness} = \exp(-LAI) \quad (21)$$

196 ~~Bareness is originally defined as $\exp(-LAI-SAI)$, where SAI is stem area index (Evans et~~
197 ~~al. 2016). Since satellite does not retrieve brownish SAI, we only use LAI to calculate~~
198 ~~bareness.~~

199 PRECL precipitation from the National Oceanic and Atmospheric Administration
200 (NOAA) is a global analysis available monthly from 1948 to present at a 1° by 1°
201 resolution. The dataset is derived from gauge observations from the Global Historical
202 Climatology Network (GHCN), version 2, and the Climate Anomaly Monitoring System
203 (CAMS) datasets. Its long coverage and ~~relatively high~~ spatial resolution is ~~quite~~ suitable
204 to study the connections between DOD and precipitation.

205

206 2.3 CMIP5 model output

207 | Among CMIP5 models we selected seven models (Table 1) that used interactive
208 | dust emission schemes, in which dust emission varied in response to changes of climate.
209 | The output of 10 m wind speed, precipitation, and LAI are also available from these
210 | models. In models that dust is simulated offline, i.e., dust emission did not interactively
211 | respond to meteorological and climate changes, the connections between DOD and
212 | modeled controlling factors are lost. Other models (to our best knowledge) either used
213 | offline dust as an input, ~~in which dust emission did not interactively respond to~~
214 | ~~meteorological and climate changes,~~ or did not write out the variables needed for this
215 | analysis.

216 | Both historical run from 1861 to 2005 and future run under the Representative
217 | Concentration Pathways 8.5 (RCP 8.5) scenario (Riahi et al., 2011) from 2006 to 2100
218 | are used. Here the RCP 8.5 scenario is chosen because it represents the upper limit of the
219 | projected greenhouse gas change in the twenty-first century and thus likely is the worst-
220 | case scenario for future DOD variation under climate change. Also, studies found that
221 | observed CO₂ emission pathway during 2005-2014 matches RCP 8.5 scenario better than
222 | other scenarios (e.g., Fuss et al., 2014), which makes the RCP8.5 output suitable to
223 | examine present-day DOD variations after 2005.

224 | Monthly model output of dust load, surface 10 m wind speed, precipitation, and
225 | LAI are used. Historical output from 2003 to 2005 and RCP 8.5 output from 2006 to
226 | 2016 are combined to form time series and climatology during 2003-2016 to compare
227 | with MODIS DOD during the same time period.

228

229 2.3.1 DOD derived from modeled dust load

230 Most CMIP5 models did not save DOD, so we used monthly dust load and
231 converted them to DOD using the relationship derived by Ginoux et al. (2012a) as the
232 following

$$233 \quad \tau = M \times e \quad , \quad (32)$$

234 where τ is DOD at 500 nm, M is the load of dust in unit of (g m^{-2}), and $e = 0.6 \text{ m}^2 \text{ g}^{-1}$ is
235 the mass extinction efficiency. Dust load from different models is first interpolated to a
236 2° by 2.5° grid and then converted to DOD. The same method was used by Pu and
237 Ginoux (2017) for the U.S. Applying the same mass extinction efficiency everywhere
238 and to all the CMIP5 model output used here is a simplification, as different models may
239 have quite different mass extinction efficiency. For instance, e can range from 0.25 to
240 $1.28 \text{ m}^2 \text{ g}^{-1}$ in AEROCOM models, with a multi-model medium of $0.72 \text{ m}^2 \text{ g}^{-1}$ (Huneus
241 et al., 2011). Here, we compared the derived DOD with modeled DOD from one
242 historical simulation of GFDL-CM3 model (Donner et al., 2011) as an example. A full
243 validation of this method will require modeled DOD from all the other CMIP5 models,
244 which are currently not available. The pattern correlation of the climatology (1861-2005)
245 between the derived DOD and modeled DOD in GFDL-CM3 are very high, all above
246 0.99 for four seasons (not shown). The percentage differences between derived DOD and
247 modeled DOD averaged over global land range from -3.6% in DJF and SON to 1.3% in
248 MAM and JJA. ~~Over Africa, DOD is slightly overestimated by 0-6.7% (regional mean),~~
249 ~~while over the Middle East, there is a small underestimation by -1.6% in SON and up to~~
250 ~~8.2% overestimation in JJA. Among the nine regions we focused in this analysis, three~~
251 ~~regions (North America, South Africa, and South America) show an underestimation of~~

252 | ~~more than 20% in some seasons and two regions (Northern China and Australia) show an~~
253 | ~~overestimation of more than 10% in some seasons.~~

254

255 | ~~2.4 Multiple linear~~ A linear regression model

256 | 2.4.1 Multiple linear regression

257 | In order to examine the relative contribution of each local controlling factor to
258 | DOD variations, multiple linear regression is applied by regressing MODIS DOD onto
259 | standardized seasonal mean ERA-Interim surface wind speed, AVHRR bareness, and
260 | PRECL precipitation at each grid point. All the data are re-gridded to a 1° by 1° grid
261 | before the calculation. Over regions where values are missing for any of the explanatory
262 | variables (i.e., precipitation, bareness, and surface wind speed) or DOD, the regression
263 | coefficients are set to missing values. The collinearity among these explanatory variables
264 | is examined by calculating variance inflation factor (VIF) (e.g., O'Brien, 2007; Abudu et
265 | al., 2011), and in most regions the VIF is below 2 (not shown), indicating a low
266 | collinearity (5–10 is usually considered high). Bootstrap resampling is used to test the
267 | significance of the regression coefficients, following the method used by Pu and Ginoux
268 | (2017).

269 | Multiple linear regression is also applied to CMIP5 model derived DOD and
270 | output of surface wind speed, bareness, and precipitation to obtain regression coefficients
271 | from the models from 2004 to 2016. All variables are interpolated to a 2° by 2.5° grid
272 | before regression. The results are compared with regression coefficients derived from
273 | observational datasets.

274

275 **2.4.2 DOD reconstruction and future projection**

276 Using regression coefficients obtained from observations and observed variations
277 of precipitation, bareness, and surface wind speed from 2004 to 2016, we can reconstruct
278 DOD in the present day and compare it with MODIS DOD (see discussion in section 3.2).

279 Similar to the method used by Pu and Ginoux (2017), the regression coefficients
280 derived from MODIS DOD and observed controlling factors ~~from 2004 to 2016~~ and
281 CMIP5 model output of surface wind speed, bareness, and precipitation are used to
282 project variations of future DOD. The regression coefficients are interpolated from the 1°
283 by 1° grid to a 2° by 2.5° grid to be consistent with model output. Such an interpolation
284 may smooth out some spatial characteristics from observations. Here we tried two groups
285 of CMIP5 output for these controlling factors. One group used seven models with
286 interactive dust emission scheme (Table 1), and the other used 16 CMIP5 models ~~as did~~
287 ~~by (see Supplementary Table S1 of Pu and Ginoux, (2017); their Supplementary Table S1)~~
288 that include the seven models with interactive dust emission scheme. The reason to test
289 the latter is to include as much model output of the controlling factors as possible. The
290 differences between the historical run (1861–2005 average) and that of the RCP 8.5 run
291 for the late half of the twenty-first century (2051–2100) are standardized by the standard
292 deviation of the historical run for each explanatory variable. The projected change reveals
293 how DOD will vary with reference to the historical conditions (mean and standard
294 deviation).

295 296 **3. Results**

297 **3.1 Climatology (2004-2016)**

298 Figure 1 shows the climatology of MODIS DOD (top panel) in four seasons
299 during 2004-2016 and that from the CMIP5 multi-model mean (bottom). Globally, the
300 dustiest regions are largely located over the northern hemisphere (NH) over North Africa,
301 the Middle East, and East Asia (Figs. 1a-d). In these regions, DOD is higher in boreal
302 spring and summer than fall and winter. Modeled global DOD over land is generally
303 lower than that from MODIS DOD, ranging from -0.028 (-25.2%) in MAM to -0.005 (-
304 6.4%) in DJF. The global spatial pattern is better captured in MAM and JJA, with pattern
305 correlations of 0.74 and 0.85, respectively (Figs. 1f-g). In DJF, DOD is overestimated
306 over central Africa and Australia, but underestimated over the Middle East and Asia (Fig.
307 1e), while in SON there is a similar overestimation in Australia and an underestimation in
308 the Middle East (Fig. 1h).

309 Figure 2 shows the zonal mean of CMIP5 DOD from individual models (thin
310 colorful lines) and multi-model ensemble mean (thick black), in comparison with MODIS
311 DOD (thick red). In DJF, DOD is underestimated in the NH from 15° N to 50°N but
312 overestimated over the tropics and southern hemisphere (SH) (Fig. 2a). While the
313 overestimation in the SH is largely contributed by three models, the underestimation in
314 the NH appears in all the seven models. The overestimation of DOD in HadGEM2-ES
315 has also been identified in a previous study (Bellouin et al., 2011) and will be discussed
316 later. In MAM, a similar overestimation of DOD in the tropics and SH also occurs in
317 some models, and the multi-model mean slightly overestimates DOD around 20°-30°S
318 (Fig. 2b). In NH, there is a weak underestimation too, but the overall gradient is largely
319 captured. In JJA, the multi-model mean resembles MODIS DOD very well (Fig. 2c),
320 consistent with the highest pattern correlation in this season shown in Fig. 1. The peak

321 around 19° N in North Africa and Middle East is well captured by the multi-model mean,
322 although the magnitude is slightly underestimated. In SON, different from MODIS DOD
323 that peaks around 19°N, the multi-model mean has two peaks around 15°N and 28°S,
324 respectively, a pattern somewhat similar to that in DJF (Fig. 2d). Consequently, DOD in
325 CMIP5 multi-model mean is overestimated at 15°-40°S and 0°-15°N but underestimated
326 at 15°S -0° and 15°-40°N.

327 Seasonal cycles of CMIP5 DOD are compared with MODIS DOD in nine regions
328 in Figure 3. The annual means of DOD in each region from multi-model mean (black)
329 and MODIS (red) are also listed in each plot. The spread of DOD among individual
330 models is greater during boreal spring and summer for regions in the NH and during
331 austral spring and summer for regions in the SH ~~than other seasons~~. Seasonal cycles over
332 North Africa, the Middle East, North America, and India are generally captured by multi-
333 model mean, with modeled DOD peaking during the same seasons as MODIS DOD
334 (Figs. 3a-b, d-e). While some models overestimate the seasonal peaks over the Middle
335 East, North America, and India (e.g., CanESM2, HadGEM2-ES, and HadGEM2-CC), a
336 few models have very weak seasonal cycles and underestimate DOD over North America
337 and India (e.g., GFDL-CM3, NorESM1-M, MIROC-ESM, and MIROC-ESM-CHEM).
338 Note that MODIS DOD is slightly lower than CALIOP DOD over India in MAM (Fig.
339 S5), therefore for these models the underestimation may be larger than shown in Fig. 3e.

340 Since the temporal coverage of MODIS DOD over northern China and
341 southeastern Asia is relatively low in JJA compared with other regions (Fig. S3), we also
342 examined the seasonal cycle of CALIOP DOD (not shown) and results are similar but
343 with weaker magnitude. Over northern China, MODIS DOD peaks in spring (Fig. 3c),

344 consistent with previous studies (e.g., Zhao et al., 2006; Laurent et al., 2006; Ginoux et
345 al., 2012b), while multi-model mean peaks ~~much~~ later in May-June. Individual models
346 have quite different seasonal cycles, with GFDL-CM3 model having a peak (in April)
347 closer to the timing of MODIS maximum. Similar misrepresentation occurs over the
348 southeastern Asia (Fig. 3f).

349 In South Africa and South America the observed maxima in early austral spring
350 (i.e., September) are also ~~missed~~ not captured by the multi-model mean (Figs. 3g-h). Note
351 that CanESM2 largely captures the seasonal cycle of DOD over South America, although
352 the magnitude is overestimated (Fig. 3h). In Australia, DOD is largely overestimated and
353 the peak from November to January in MODIS DOD is ~~also misrepresented in the~~ shifted
354 about one month earlier in the multi-model mean (Fig. 3i). Similar to the finding here,
355 Bellouin et al. (2011) also found that HadGEM2-ES model overestimated DOD over
356 Australia and Thar desert region in northwestern India and suggested that these
357 overestimations were likely due to model's overestimation of bare soil fraction and
358 underestimation of soil moisture. Despite overestimation, the seasonal cycle in
359 HadGEM2-CC model is more similar to MODIS DOD than other models (Fig. 3i).

360 We further examine the magnitudes and spatial patterns of CMIP5 DOD in these
361 regions. Figure 4 shows the ratio of pattern standard deviations (standard deviations of
362 values within the domain) and pattern correlation between CMIP5 DOD and MODIS
363 DOD climatology (2004-2016) in each region for four seasons. While the former reveals
364 the magnitude differences, the latter demonstrates the spatial resemblance.

365 Over North Africa, the Middle East, and India, the ratio of CMIP5 DOD from
366 individual models and multi-model mean versus MODIS DOD are all within \pm one order

367 of magnitude (Fig. 4). Most models underestimate DOD in northern China, although the
368 magnitudes are largely within the range of -one order of magnitude to one. Over North
369 America, South Africa, and Australia, some models underestimate the DOD by more than
370 two orders of magnitudes, while over Australia three models overestimate DOD by more
371 than one order of magnitude. In general, magnitudes of multi-model mean are closer to
372 satellite DOD than most individual models and are largely within \pm one order of
373 magnitude of MODIS DOD.

374 The spatial patterns are better captured over North Africa and the Middle East
375 than other regions (Fig. 4), with pattern correlations above 0.6 in most models (with
376 highest pattern correlation of 0.92 and 0.83, respectively). Pattern correlations from
377 multi-model mean are also high, reaching 0.87 (0.78) over North Africa and 0.75 (0.73)
378 over the Middle East in JJA (MAM). Nonetheless, some models show negative pattern
379 correlations over North Africa, northern China, North America, southeastern Asia, South
380 Africa, South America, and Australia. Overall, spatial patterns are less well represented
381 in regions over the SH than over the NH in CMIP5 models.

382 In short, in terms of both magnitudes and spatial pattern, DOD climatology is best
383 represented over North Africa and the Middle East among the nine regions. The multi-
384 model mean shows that DOD over North Africa is slightly better simulated than over the
385 Middle East, somewhat similar to the finding of AeroCom multi-model analysis
386 (Huneus et al. 2011).

387

388 **3.2 Interannual variations**

389 | An important aspect of dust activity is its long-term ~~variability~~variations,
390 | including interannual and decadal variations. Dust emission in North Africa is known to
391 | have strong decadal variations (e.g., Prospero and Nees, 1986; Prospero and Lamb, 2003;
392 | Mahowald et al., 2010; Evan et al., 2014, 2016), while over Australia, strong interannual
393 | variations have been related to El Niño–Southern Oscillation (e.g., Marx et al., 2009;
394 | Evans et al., 2016). Due to the short time coverage of high quality satellite products, we
395 | focus on interannual variations of DOD from 2004 to 2016.

396 | Figure 5 shows the correlations of regional mean time series of DOD between
397 | MODIS and CMIP5 models and multi-model mean for each season in nine regions. We
398 | also show correlations between the reconstructed DOD (see section 2.4.2 for details) and
399 | MODIS DOD for reference (Table S1 in the Supplement). ~~Previous study found that the
400 | variations of dust event frequency over the U.S. in the recent decade could be largely
401 | represented by the variations of three local controlling factors: seasonal mean surface
402 | wind speed, bareness, and precipitation (Pu and Ginoux, 2017). These factors have
403 | previously been found to constrain dust emission or variability on multiple time scales
404 | (e.g., Gillette and Passi, 1988; Fecan et al., 1999; Zender and Kwon, 2005). While
405 | surface wind is positively related to the emission and transport of dust, vegetation is an
406 | important non-erodible element that prevents soil erosion from wind. Precipitation is
407 | generally negatively related to dust emission and transport processes. While the
408 | scavenging effect of precipitation on small dust particles only lasts a few hours or days,
409 | influences of precipitation on soil moisture lasts longer. Here we extend our regression
410 | model (Pu and Ginoux, 2017) to a global scale. Regression coefficients are obtained by
411 | regressing MODIS DOD onto observed surface wind, bareness, and precipitation during~~

412 | ~~2004-2016 (see methodology section for details).~~ The reconstructed DOD is ~~then~~
413 | calculated using ~~these observed~~ regression coefficients and time-varying controlling
414 | factors from observations (i.e., surface wind speed, bareness, and precipitation).

415 | The interannual variations of DOD are in general not well captured by CMIP5
416 | models. This is consistent with previous study by Evan et al. (2014) who found dust
417 | variability downwind of North Africa over the northeastern Atlantic was misrepresented
418 | in CMIP5 models. In most regions, only one or two models show significant positive
419 | correlation with MODIS DOD in some seasons, and negative correlations exist in all
420 | regions (Fig. 5). North Africa, the Middle East, southeastern Asia, South America, and
421 | Australia show less negative correlations than other dusty regions. On the other hand,
422 | reconstructed DOD shows significant positive correlations with MODIS DOD over most
423 | regions in all seasons (Table S1 in the Supplement). This suggests that the interannual
424 | variations of DOD can be largely attributed to the variations of these controlling factors,
425 | and models ~~probably may misrepresented~~ these relationships, in addition to their
426 | incapacity of capturing the interannual variations of individual controlling factors in
427 | general (~~Figures S4-6 in the Supplement not shown~~), which is not uncommon for coupled
428 | models.

429 | We further examine the connection between those controlling factors and DOD in
430 | CMIP5 models. Figure 6 shows the dominant controlling factors among the three (surface
431 | wind speed, bareness, and precipitation) on DOD variations in four seasons from MODIS
432 | (left column) and from CMIP5 multi-model mean (right column), respectively. To
433 | highlight factors controlling DOD variations near the dust source regions, a mask of
434 | AVHRR LAI \leq 0.5 is applied to both coefficients.

435 Bareness plays the most important role in many dusty regions in observations,
436 e.g., over Australia, central U.S., and South America (Figs. 6a-d). Note that while
437 bareness plays an important role over the Sahel during DJF and MAM, it also shows
438 strong signal over some areas in the northern North Africa (Figs. 6a-b). The reliability of
439 this information is limited by the accuracy of LAI retrieval in these areas. The value of
440 bareness in this region is actually quite high (as LAI is very low), but still has weak
441 interannual variability (Figures S67 in the Supplement). Over some areas of North and
442 South Africa, the Middle East, and East Asia, surface wind and precipitation are also
443 quite important.

444 The role of bareness is largely underestimated in CMIP5 models, while surface
445 wind and precipitation become the dominant factors (Figs. 6e-h). The misrepresentation
446 of the connection between DOD and these controlling factors may cause the
447 misrepresentation of the dust load and its variability. Taking Australia for an example,
448 the overestimation of DOD magnitudes may be related to an overestimation of the
449 influence of surface wind on DOD and a lack of constraints from surface bareness.

450 Despite the large differences between the observed and modeled connections
451 between DOD and the controlling factors, some regions show similarities. For instance,
452 over North Africa in DJF, both show an important influence from surface winds (Figs.
453 6a, e), although the locations of surface wind-dominant areas are not exactly the same.
454 Evan et al. (2016) also found a dominant role of surface wind on African dust variability,
455 but they focused on monthly means, not seasonal averages. In MAM, precipitation starts
456 to play a role in some parts of North Africa, while surface wind still dominates in some
457 areas (Fig. 6b). Same increasing influence of precipitation is shown in the multi-model

458 mean, but such an influence seems overestimated (Fig. 6f). In JJA, the influences of
459 ~~surface wind in North Africa and~~ precipitation and bareness over the eastern Arabian
460 Peninsula in the Middle East in the multi-model mean (Fig. 6g) also show some similarity
461 to observation (Fig. 6c), although an underestimation of the influence from bareness and
462 an overestimation of ~~surface wind~~precipitation are still there.

463 Also, note that in CMIP5 models, due to lack of constraints from low surface
464 temperature (e.g., over frozen land) and snow cover on dust emission or
465 misrepresentations of dust transport, DOD and also the regression coefficients still exist
466 over NH high latitudes in boreal winter and spring in the multi-model mean (Figs. 6e-f).

467

468 **3.3 Future projections**

469 How will DOD change in response to increasing greenhouse gases? The results
470 from CMIP5 multi-model mean are shown in Figure 7. We compare the DOD during the
471 late half of the 21st century under the RCP 8.5 scenario with that in the historical level
472 (1861-2005 average).

473 Over land, CMIP5 model projects a decrease of global mean DOD in all seasons
474 except JJA (Figs. 7a-d). The inter-model standard deviation is much greater than the
475 multi-model mean, suggesting large discrepancies among individual models. The
476 projected decrease is largely over northern North America, southern North Africa, eastern
477 central Africa, and East Asia, while the increase is largely over northern North Africa, the
478 Middle East, southern North America, South Africa, South America, and southern
479 Australia (Fig. 7). Regional means of DOD change (in percentage) with reference to
480 CMIP5 historical run are summarized in Table 3.

481 What might be the causes of DOD change? Figure 8 shows the projected change
482 of precipitation, bareness, and surface wind speed from CMIP5 multi-model mean. These
483 factors play important role in DOD variations in the present day, although models tend to
484 underestimate the role of bareness and overestimate the influences of precipitation and
485 surface wind (Fig. 6). Increases in precipitation can increase soil moisture and remove
486 airborne dust, thus usually favors a decrease of DOD. As shown in Figs. 8a-d, the
487 increases of precipitation in northern Eurasia, northern North America, the Congo basin
488 in Africa, and Australia (DJF and MAM) may contribute to the decrease of DOD in these
489 regions, while the decreases of precipitation over northern North Africa and the Middle
490 East (DJF and MAM), South Africa, and South America may contribute to the increase of
491 DOD (DJF-SON). Also note that in JJA both precipitation and DOD increase over
492 northern North Africa and the Middle East (Fig. 8c), suggesting other factors dominate
493 the variation of DOD in the multi-model mean.

494 A decrease (increase) of bareness indicates a growth (decay) of vegetation and is
495 usually associated with a decrease (increase) of DOD. In general, except regions such as
496 southern North America, South America, South Africa, part of northern Eurasia, and
497 central Sahel, the pattern of bareness change does not resemble DOD change (Figs. 8e-h).
498 This is probably due to the fact that the overall influence of bareness on DOD variation is
499 underestimated in CMIP5 models (Fig. 6).

500 Increases in surface wind can enhance dust emission and transport, and vice versa.
501 The changes of surface wind in DJF and MAM are similar and likely to contribute to the
502 increase of DOD over northern North Africa, the Middle East, eastern South America,
503 | southern South Africa, and southern Australia (Figs. 8i-j). The decrease of DOD over

504 northwestern North America, the Sahel, and northern Australia may also relate to the
505 decrease of surface wind there, in addition to an increase of precipitation and a reduction
506 of bareness. In JJA and SON (Figs. 8k-l), the increases of surface wind in South America,
507 South Africa, central Australia and the decreases of wind in northwestern North America,
508 northern Eurasia, and the central Sahel are also consistent with patterns of DOD change.

509 In short, variations of CMIP5 DOD in the late half of the 21st ~~century~~ ~~centaury~~
510 are more consistent with changes of precipitation and surface wind speed than with
511 surface bareness, consistent with the analysis above regarding to the present-day
512 condition.

513 ~~Here we also present t~~The projected change of DOD from the regression model ~~is~~
514 ~~shown in~~ Figure 9. ~~The regression model (see section 2.4 for details) is developed based~~
515 ~~on observed relationships between MODIS DOD and local controlling factors and can~~
516 ~~largely capture the interannual variations of DOD in the present-day climate (Table S1 in~~
517 ~~the Supplement). Assuming that the observed connection between DOD and these~~
518 ~~controlling factors do not change dramatically in the future, we can use this regression~~
519 ~~model and CMIP5-model projected change of controlling factors to project DOD~~
520 ~~variations. Compared to DOD projection from CMIP5 models, this approach utilizes~~
521 ~~additionally observational constrains and is likely to provide a more reliable future~~
522 ~~projection. The results are calculated using~~We use the regression coefficients obtained
523 ~~from observations during 2004-2016 and~~ projected changes of precipitation, bareness,
524 and surface wind speed from ~~seven~~16 CMIP5 models ~~with interactive dust emission~~
525 ~~scheme~~ (see methodology). A similar method is applied to the model output from ~~seven~~
526 ~~16~~ CMIP5 models ~~with interactive dust emission scheme~~, and results are similar (Figure

527 | [S78](#) in the Supplement). A mask of present-day LAI ≤ 0.5 is also applied to highlight the
528 | changes of DOD near dust source regions. By doing this, we assume the location of
529 | major dust sources will not change much at the late half of the 21st century. The
530 | unmasked figure is presented in the supplementary file (Figure [S89](#) in the Supplement).
531 | The reason we did not use the projected future LAI as a mask is that there're large
532 | uncertainties associated with LAI projection, especially over northern hemisphere
533 | subtropical regions (e.g., Figs. 8e-h).

534 | In DJF, regression model projected change of DOD over Mexico, North Africa,
535 | the Middle East and part of northern China (Fig. 9a) are similar to those projected by
536 | CMIP5 models over those dust source regions (Fig. 7a), but with a greater magnitude. In
537 | MAM, a decrease of DOD is projected over large area of North Africa (Fig. 9b), which is
538 | different from the pattern projected from the CMIP5 multi-model mean (Fig. 7b). The
539 | decrease of DOD over northern central U.S. is also different from the overall increase
540 | projected by CMIP5 DOD, ~~as also noted by Pu and Ginoux (2017)~~. However, the
541 | increase of DOD over the Middle East and the decrease of DOD over northern China are
542 | similar to that of CMIP5 DOD. During JJA and SON, DOD decreases over the Sahel and
543 | northern China but increases over a belt to the north of central Sahel and parts of the
544 | Middle East (Figs. 9c-d). The weak increase of DOD over the southern corner of South
545 | Africa in JJA and a slight decrease in SON also has high agreement among the
546 | ~~models~~regression projections (dotted areas in Figs. 9c-d). Changes of DOD over
547 | Australia are very small in all seasons and show little consistency among the ~~models~~
548 | regression projections.

549 The regression model projection using 16-model output shows very similar
550 patterns (Figure S7 in the Supplement), largely because the projected changes of
551 precipitation, surface wind speed, and bareness from 16-model ensemble mean are
552 similar to those from 7-model ensemble mean in dusty regions (Figure S9 in the
553 Supplement). But there are also some discrepancies in terms of magnitude and pattern
554 that are revealed in the projected DOD patterns, e.g., the projected reduction of DOD is
555 greater and more widespread over the northern Asia in MAM if using 16-model output
556 and the increase of DOD along the southern edge of the Sahara is weaker in JJA and
557 SON (Fig. S7 in the Supplement vs. Fig. 9).

558 The contribution of each controlling factor to the total DOD change is shown in
559 Figure 10. While changes of bareness over North Africa, ~~northern Middle East~~ and
560 northern China play an important role in DOD change, changes of precipitation, e.g. over
561 northwestern China in MAM, and surface wind, e.g., over northern North Africa and the
562 Middle East in DJF and MAM, also play vital roles.

563 Both projections from the CMIP5 models and that from the regression model have
564 large-some uncertainties. The reliability of future projection by CMIP5 models is limited
565 by models' capability of capturing present-day climatology and observed connection
566 between DOD and local controlling factors. As discussed earlier, the overall performance
567 of models is better in those very dusty regions in the NH, such as North Africa and the
568 Middle East, than other regions. Multi-model mean also overestimates the connection
569 between DOD and precipitation and surface wind and underestimates the influence of
570 bareness in the present-day (Fig. 6), which can cast doubts on the projected variation of
571 DOD in response to climate change.

572 The uncertainties associated with regression model are two folds. First, there're
573 uncertainties associated with the regression model itself. Since the regression coefficients
574 are derived from observed relationships between DOD and controlling factors in a
575 relatively short time period, factors controlling the low frequency variation of DOD (e.g.,
576 decadal variations) may not be included. Other meteorological factors that could play an
577 important role in regional dust variability, e.g., nocturnal low-level jets (e.g., Todd et al.,
578 2008; Fiedler et al., 2013; Fiedler et al., 2016) and haboobs over Africa (e.g., Ashpole
579 and Washington, 2013), are not directly considered in the model. The influences of
580 anthropogenic land use/land cover change are also not included in the regression model.
581 Anthropogenic land use/land cover change has been found to have played an important
582 role in long-term dust variability in some regions (e.g., Neff et al., 2005; 2008; Moulin
583 and Chiapello, 2006; McConnell et al., 2007), although previous modeling study found
584 its influences on future dust emission was minor compared to climate change (Tegen et
585 al., 2004). So the projection made by the regression model only reveals the change of
586 DOD in association with climate change. Second, uncertainties associated with model
587 projected change of controlling factors, such as bareness in U.S. in JJA as pointed by Pu
588 and Ginoux (2017), also limit the accuracy of the results.

589 Despite these uncertainties, both methods make similar projections particularly in
590 some dusty regions. For instance, the DOD pattern over North Africa in DJF and JJA, an
591 increase of DOD in the [central](#) Arabian Peninsula in all seasons, and a decrease of DOD
592 over northern China from MAM to SON (Figs. 7, 9).

593

594 **4. Discussion**

595 We examined DOD in seven CMIP5 models with interactive dust emission
596 schemes. Other important variables that influence the radiative property ~~and~~
597 ~~concentration~~ of dust, such as Angström exponent and single scattering albedo, ~~dust~~
598 ~~emission, and surface concentration~~, are also worth further examination, if these variables
599 are archived. A better quantification of the radiative forcing of dust may also require an
600 examination on the size distribution of dust particles, as studies (e.g., Kok et al., 2017)
601 found in current AeroCom models fraction of coarse dust particles were underestimated
602 and so was the warming effect of dust. Whether this is the case in the CMIP5 models is
603 not clear.

604 Also note that since DOD is an integrated variable, it does not reflect the vertical
605 distribution of dust aerosols. As pointed by Huneus et al., (2016), dust models with
606 similar performance in simulating aerosol optical depth may have quite large differences
607 in simulating vertical distribution, emission, deposition, and surface concentration of
608 dust. An overall evaluation of dust modeling capability will require detailed examination
609 of these variables and the life cycle of dust in CMIP5 models in addition to DOD.

610 Early studies on future dust projection used offline dust models driven by climate
611 model output under different scenarios. For instance, Mahowald and Luo (2003) used an
612 offline dust model and output from National Center of Atmospheric Research's coupled
613 Climate System Model (CSM) 1.0 (Boville and Gent, 1998) under A1 scenario
614 (Houghton et al., 2001) and projected a decrease of dust emission by the end of the 21st
615 century by -20% to -63%, depending on different scenarios. In general, when they
616 included vegetation change, the projected dust reduction became greater, but including
617 land use change slightly weakened such reduction. Similarly, Tegen et al. (2004) used

618 output from ECHAM4 and HadCM3 and a dust model (Tegen et al., 2002) to examine
619 the change of dust emission by 2040-2050 and 2070-2080 and found results were model
620 and scenario dependent, from -26% to 10%. However, including anthropogenic
621 cultivation practices tended to increase dust emission in both models. They also pointed
622 out that such an influence from anthropogenic land-use was not big enough to overcome
623 the effect of climate change.

624 The interactive dust emission schemes and new generations of climate models
625 used in CMIP5 are likely to provide more reliable projections, but this may also depend
626 on how changes of dust and its radiative forcing are fed back to the climate system in the
627 models. While these projections are largely model-dependent, based on our analysis on
628 the DOD climatology in CMIP5 models, the multi-model mean has a better chance to
629 provide a more reliable projection than individual models.

630 Here a regression model combined with MODIS DOD is used to identify key
631 local factors that control the variation of DOD on the interannual time scale. The results
632 are then compared with model output to examine models' capability of capturing
633 observed connections between DOD and controlling factors. This method may be applied
634 to other dust model intercomparison projects as well, such as AeroCom (Huneus et al.
635 2011), to help examine model performance.

636

637 **5. Conclusion**

638 Dust aerosol plays an important role in the climate system by directly scattering
639 and absorbing solar and longwave radiation and indirectly affecting the formation and
640 radiative properties of cloud. It is thus very important to understand how well dust is

641 simulated in the state-of-the-art climate models. While many features and variables are
642 systematically examined in the CMIP5 multi-model output, we found that to our best
643 knowledge an evaluation of global dust modeling in CMIP5 models is still in blank. In
644 this study we examined a key variable associated with dust radiative effect, dust optical
645 depth (DOD), using seven CMIP5 models with interactive dust emission schemes and
646 DOD retrieved from MODIS Deep Blue aerosol products.

647 We found that the global spatial pattern and magnitude are largely captured by
648 CMIP5 models in the 2004-2016 climatology, with an underestimation of global DOD
649 (over land) by -25.2% in MAM to -6.4% in DJF. The spatial pattern is better captured in
650 boreal dusty seasons during MAM and JJA. In JJA, the simulated zonal mean DOD from
651 multi-model mean largely captures-resembles MODIS DOD ~~quite well~~.

652 The magnitudes of multi-model mean are closer to MODIS climatology than most
653 individual models and are largely within \pm one order of magnitude of MODIS DOD in
654 the nine regions examined here (North Africa, the Middle East, ~~n~~Northern China, North
655 America, India, southeastern Asia, South Africa, South America, and Australia; see Fig. 1
656 and Table 2 for domains). While some models underestimate DOD in North America and
657 South America by more than two orders of magnitude, a few also overestimate DOD in
658 Australia by more than one order of magnitude. Both the magnitude and spatial patterns
659 of DOD are better captured over North Africa and the Middle East than other regions.

660 The multi-model mean also largely captures the seasonal cycle of DOD in some
661 very dusty regions, such as North Africa and the Middle East. Seasonal variations in
662 North America and India are also generally captured by the multi-model mean, with the
663 modeled DOD peaking at approximately the same season as in MODIS DOD, but not so

664 | in northern China and southeastern Asia. Seasonal cycles in those dusty regions in the
665 | southern hemisphere is generally not well captured, with modeled DOD over South
666 | Africa and South America peaking later than that in MODIS DOD but earlier in
667 | Australia.

668 | The interannual variations of DOD are not captured by most of the CMIP5
669 | models during 2004-2016. ~~This is likely due to models' underestimation~~
670 | ~~underestimate of~~ the constraints from surface bareness on ~~the variations of dust~~ DOD and
671 | ~~overestimation of~~ the influences from surface wind speed and precipitation in those
672 | major dust source regions, ~~in addition to the fact that coupled models usually do not~~
673 | ~~capture the observed interannual variations of precipitation, surface wind, and bareness as~~
674 | ~~well~~. CMIP5 model projected change of DOD in the late half of the 21st century (under
675 | the RCP 8.5 scenario) with reference to historical condition (1861-2005) also shows
676 | greater influence from precipitation and surface wind change than from surface bareness.
677 | Overall, multi-model mean projects a change of DOD over land from -3.8% in SON to
678 | 3.3% in JJA.

679 | We also provide a projection of future DOD change using a regression model
680 | based on local controlling factors such as surface wind, bareness, and precipitation (Pu
681 | and Ginoux, 2017). This model can largely capture the interannual variations of MODIS
682 | DOD in 2004-2016. The regression model projects a reduction of DOD in the Sahel in all
683 | seasons in the late half of the 21st century under the RCP 8.5 scenario, largely due to a
684 | decrease of surface bareness. DOD is projected to increase over the southern edge of the
685 | Sahara in association with surface wind and precipitation changes except in MAM, when
686 | a reduction of DOD over most part of North Africa is projected. DOD is also projected

687 | to increase over the central Arabian Peninsula in all seasons and to decrease over
688 | northern China from MAM to SON.

689 | Despite large uncertainties associated with both projections, we find some
690 | similarities between the two, ~~which may be informative,~~ which adds to the confidence of
691 | projected DOD change in these regions, for instance, changes of DOD over North Africa
692 | in DJF and JJA, an increase of DOD in the central Arabian Peninsula in all seasons, and a
693 | decrease of DOD over northern China from MAM to SON.

694

695

696

697

698

699

700

701

702

703

704

705

706

707

708

709 |

710 *Acknowledgements.*

711 This research is supported by NOAA and Princeton University's Cooperative
712 Institute for Climate Science and NASA under grant NNH14ZDA001N-ACMAP. The
713 authors thank Drs. Songmiao Fan and Fabien Paulot for their helpful comments on the
714 early version of this paper. [The insightful comments from two anonymous reviewers](#)
715 [improved the paper.](#)

716 PRECL Precipitation data are provided by the NOAA/OAR/ESRL PSD, Boulder,
717 Colorado, USA, from their web site at <http://www.esrl.noaa.gov/psd/>. The CALIOP
718 products are downloaded from [https://www-](https://www-calipso.larc.nasa.gov/tools/data_avail/dpo_read.php?y=2007&m=08&d=10)
719 [calipso.larc.nasa.gov/tools/data_avail/dpo_read.php?y=2007&m=08&d=10](https://www-calipso.larc.nasa.gov/tools/data_avail/dpo_read.php?y=2007&m=08&d=10). AVHRR
720 leaf area index data are available at:

721 [https://www.ngdc.noaa.gov/docucomp/page?xml=NOAA/NESDIS/NCDC/Geoportal/iso/](https://www.ngdc.noaa.gov/docucomp/page?xml=NOAA/NESDIS/NCDC/Geoportal/iso/xml/C00898.xml&view=getDataView&header=none)
722 [xml/C00898.xml&view=getDataView&header=none.](https://www.ngdc.noaa.gov/docucomp/page?xml=NOAA/NESDIS/NCDC/Geoportal/iso/xml/C00898.xml&view=getDataView&header=none)

723 ftp://eclipse.nedc.noaa.gov/pub/edr/lai_fapar/files/. The ERA-Interim is downloaded
724 from <http://www.ecmwf.int/en/research/climate-reanalysis/era-interim>. The AERONET
725 coarse mode aerosol optical depth data are downloaded from
726 <https://aeronet.gsfc.nasa.gov/>. CMIP5 data are downloaded from:

727 <https://pcmdi.llnl.gov/projects/esgf-llnl/>.

728

729

730

731

732

Reference

- 733
734
735 Abudu, S., Cui, C. L., King, J. P., Moreno, J., and Bawazir, A. S.: Modeling of daily pan
736 evaporation using partial least squares regression, *Sci China Technol Sc*, 54, 163-
737 174, 10.1007/s11431-010-4205-z, 2011.
- 738 Arora, V. K., Scinocca, J. F., Boer, G. J., Christian, J. R., Denman, K. L., Flato, G. M.,
739 Kharin, V. V., Lee, W. G., and Merryfield, W. J.: Carbon emission limits required
740 to satisfy future representative concentration pathways of greenhouse gases,
741 *Geophys Res Lett*, 38, 10.1029/2010gl046270, 2011.
- 742 Ashpole, I., and Washington, R.: A new high-resolution central and western Saharan
743 summertime dust source map from automated satellite dust plume tracking, *J*
744 *Geophys Res-Atmos*, 118, 6981-6995, 10.1002/jgrd.50554, 2013.
- 745 Baddock, M. C., Ginoux, P., Bullard, J. E., and Gill, T. E.: Do MODIS-defined dust
746 sources have a geomorphological signature?, *Geophys Res Lett*, 43, 2606-2613,
747 10.1002/2015gl067327, 2016.
- 748 Bangert, M., Nenes, A., Vogel, B., Vogel, H., Barahona, D., Karydis, V. A., Kumar, P.,
749 Kottmeier, C., and Blahak, U.: Saharan dust event impacts on cloud formation
750 and radiation over Western Europe, *Atmos Chem Phys*, 12, 4045-4063,
751 10.5194/acp-12-4045-2012, 2012.
- 752 Bellouin, N., Rae, J., Jones, A., Johnson, C., Haywood, J., and Boucher, O.: Aerosol
753 forcing in the Climate Model Intercomparison Project (CMIP5) simulations by
754 HadGEM2-ES and the role of ammonium nitrate, *J Geophys Res-Atmos*, 116,
755 10.1029/2011jd016074, 2011.

756 Bentsen, M., Bethke, I., Debernard, J. B., Iversen, T., Kirkevåg, A., Seland, O., Drange,
757 H., Roelandt, C., Seierstad, I. A., Hoose, C., and Kristjansson, J. E.: The
758 Norwegian Earth System Model, NorESM1-M - Part 1: Description and basic
759 evaluation of the physical climate, *Geosci Model Dev*, 6, 687-720, 10.5194/gmd-
760 6-687-2013, 2013.

761 Boville, B. A., and Gent, P. R.: The NCAR Climate System Model, version one, *J*
762 *Climate*, 11, 1115-1130, Doi 10.1175/1520-
763 0442(1998)011<1115:Tncsmv>2.0.Co;2, 1998.

764 Chen, M. Y., Xie, P. P., Janowiak, J. E., and Arkin, P. A.: Global land precipitation: A
765 50-yr monthly analysis based on gauge observations, *J Hydrometeorol*, 3, 249-
766 266, Doi 10.1175/1525-7541(2002)003<0249:Glpaym>2.0.Co;2, 2002.

767 Claverie, M., Matthews, J. L., Vermote, E. F., and Justice, C. O.: A 30+ Year AVHRR
768 LAI and FAPAR Climate Data Record: Algorithm Description and Validation,
769 *Remote Sens-Basel*, 8, 10.3390/rs8030263, 2016.

770 Collins, W. J., Bellouin, N., Doutriaux-Boucher, M., Gedney, N., Halloran, P., Hinton,
771 T., Hughes, J., Jones, C. D., Joshi, M., Liddicoat, S., Martin, G., O'Connor, F.,
772 Rae, J., Senior, C., Sitch, S., Totterdell, I., Wiltshire, A., and Woodward, S.:
773 Development and evaluation of an Earth-System model-HadGEM2, *Geosci*
774 *Model Dev*, 4, 1051-1075, 10.5194/gmd-4-1051-2011, 2011.

775 Cook, B. I., Miller, R. L., and Seager, R.: Dust and sea surface temperature forcing of the
776 1930s "Dust Bowl" drought, *Geophys Res Lett*, 35, 10.1029/2008gl033486, 2008.

777 Cook, B. I., Miller, R. L., and Seager, R.: Amplification of the North American "Dust
778 Bowl" drought through human-induced land degradation, *P Natl Acad Sci USA*,
779 106, 4997-5001, 10.1073/pnas.0810200106, 2009.

780 Cook, B. I., Seager, R., Miller, R. L., and Mason, J. A.: Intensification of North
781 American Megadroughts through Surface and Dust Aerosol Forcing, *J Climate*,
782 26, 4414-4430, 10.1175/Jcli-D-12-00022.1, 2013.

783 Croft, B., Lohmann, U., and von Salzen, K.: Black carbon ageing in the Canadian Centre
784 for Climate modelling and analysis atmospheric general circulation model, *Atmos*
785 *Chem Phys*, 5, 1931-1949, 2005.

786 Donner, L. J., Wyman, B. L., Hemler, R. S., Horowitz, L. W., Ming, Y., Zhao, M., Golaz,
787 J. C., Ginoux, P., Lin, S. J., Schwarzkopf, M. D., Austin, J., Alaka, G., Cooke, W.
788 F., Delworth, T. L., Freidenreich, S. M., Gordon, C. T., Griffies, S. M., Held, I.
789 M., Hurlin, W. J., Klein, S. A., Knutson, T. R., Langenhorst, A. R., Lee, H. C.,
790 Lin, Y. L., Magi, B. I., Malyshev, S. L., Milly, P. C. D., Naik, V., Nath, M. J.,
791 Pincus, R., Ploshay, J. J., Ramaswamy, V., Seman, C. J., Shevliakova, E., Sirutis,
792 J. J., Stern, W. F., Stouffer, R. J., Wilson, R. J., Winton, M., Wittenberg, A. T.,
793 and Zeng, F. R.: The Dynamical Core, Physical Parameterizations, and Basic
794 Simulation Characteristics of the Atmospheric Component AM3 of the GFDL
795 Global Coupled Model CM3, *J Climate*, 24, 3484-3519, 10.1175/2011jcli3955.1,
796 2011.

797 Dunion, J. P., and Velden, C. S.: The impact of the Saharan air layer on Atlantic tropical
798 cyclone activity, *B Am Meteorol Soc*, 85, 353-+, 10.1175/Bams-85-3-353, 2004.

799 Evan, A. T., Dunion, J., Foley, J. A., Heidinger, A. K., and Velden, C. S.: New evidence
800 for a relationship between Atlantic tropical cyclone activity and African dust
801 outbreaks, *Geophys Res Lett*, 33, 10.1029/2006gl026408, 2006.

802 Evan, A. T., and Mukhopadhyay, S.: African Dust over the Northern Tropical Atlantic:
803 1955-2008, *J Appl Meteorol Clim*, 49, 2213-2229, 10.1175/2010jamc2485.1,
804 2010.

805 Evan, A. T., Flamant, C., Fiedler, S., and Doherty, O.: An analysis of aeolian dust in
806 climate models, *Geophys Res Lett*, 41, 5996-6001, 10.1002/2014gl060545, 2014.

807 Evan, A. T., Flamant, C., Gaetani, M., and Guichard, F.: The past, present and future of
808 African dust, *Nature*, 531, 493-+, 10.1038/nature17149, 2016.

809 Evans, S., Ginoux, P., Malyshev, S., and Shevliakova, E.: Climate-vegetation interaction
810 and amplification of Australian dust variability, *Geophys Res Lett*, 43, 11823-
811 11830, 10.1002/2016gl071016, 2016.

812 Fecan, F., Marticorena, B., and Bergametti, G.: Parametrization of the increase of the
813 aeolian erosion threshold wind friction velocity due to soil moisture for arid and
814 semi-arid areas, *Ann Geophys-Atm Hydr*, 17, 149-157, DOI
815 10.1007/s005850050744, 1999.

816 Fiedler, S., Schepanski, K., Heinold, B., Knippertz, P., and Tegen, I.: Climatology of
817 nocturnal low-level jets over North Africa and implications for modeling mineral
818 dust emission, *J Geophys Res-Atmos*, 118, 6100-6121, 10.1002/jgrd.50394, 2013.

819 Fiedler, S., Knippertz, P., Woodward, S., Martin, G. M., Bellouin, N., Ross, A. N.,
820 Heinold, B., Schepanski, K., Birch, C. E., and Tegen, I.: A process-based

821 evaluation of dust-emitting winds in the CMIP5 simulation of HadGEM2-ES,
822 Clim Dynam, 46, 1107-1130, 10.1007/s00382-015-2635-9, 2016.

823 Fung, I. Y., Meyn, S. K., Tegen, I., Doney, S. C., John, J. G., and Bishop, J. K. B.: Iron
824 supply and demand in the upper ocean, Global Biogeochem Cy, 14, 281-295, Doi
825 10.1029/1999gb900059, 2000.

826 Fuss, S., Canadell, J. G., Peters, G. P., Tavoni, M., Andrew, R. M., Ciais, P., Jackson, R.
827 B., Jones, C. D., Kraxner, F., Nakicenovic, N., Le Quere, C., Raupach, M. R.,
828 Sharifi, A., Smith, P., and Yamagata, Y.: COMMENTARY: Betting on negative
829 emissions, Nat Clim Change, 4, 850-853, DOI 10.1038/nclimate2392, 2014.

830 Gillette, D. A., and Passi, R.: Modeling Dust Emission Caused by Wind Erosion, J
831 Geophys Res-Atmos, 93, 14233-14242, DOI 10.1029/JD093iD11p14233, 1988.

832 Ginoux, P., Chin, M., Tegen, I., Prospero, J. M., Holben, B., Dubovik, O., and Lin, S. J.:
833 Sources and distributions of dust aerosols simulated with the GOCART model, J
834 Geophys Res-Atmos, 106, 20255-20273, Doi 10.1029/2000jd000053, 2001.

835 Ginoux, P., Garbuzov, D., and Hsu, N. C.: Identification of anthropogenic and natural
836 dust sources using Moderate Resolution Imaging Spectroradiometer (MODIS)
837 Deep Blue level 2 data, J Geophys Res-Atmos, 115, 10.1029/2009jd012398,
838 2010.

839 Ginoux, P., Clarisse, L., Clerbaux, C., Coheur, P. F., Dubovik, O., Hsu, N. C., and Van
840 Damme, M.: Mixing of dust and NH₃ observed globally over anthropogenic dust
841 sources, Atmos Chem Phys, 12, 7351-7363, 10.5194/acp-12-7351-2012, 2012a.

842 Ginoux, P., Prospero, J. M., Gill, T. E., Hsu, N. C., and Zhao, M.: Global-Scale
843 Attribution of Anthropogenic and Natural Dust Sources and Their Emission Rates

844 Based on MODIS Deep Blue Aerosol Products, *Rev Geophys*, 50,
845 10.1029/2012rg000388, 2012b.

846 Houghton, J., Ding, Y., Griggs, D. J., Noguer, M., Linden, P. J. v. d., Dai, X., Maskell,
847 K., and Johnson, C. A.: Climate Change 2001: The scientific basis. Contribution
848 of Working Group I to the Third Assessment Report of the Intergovernmental
849 Panel on Climate Change, in, Cambridge Univ. Press, Cambridge, UK, 2001.

850 Hsu, N. C., Tsay, S. C., King, M. D., and Herman, J. R.: Aerosol properties over bright-
851 reflecting source regions, *Ieee T Geosci Remote*, 42, 557-569,
852 10.1109/Tgrs.2004.824067, 2004.

853 Hsu, N. C., Tsay, S. C., King, M. D., and Herman, J. R.: Deep blue retrievals of Asian
854 aerosol properties during ACE-Asia, *Ieee T Geosci Remote*, 44, 3180-3195,
855 10.1109/Tgrs.2006.879540, 2006.

856 Hsu, N. C., Jeong, M. J., Bettenhausen, C., Sayer, A. M., Hansell, R., Seftor, C. S.,
857 Huang, J., and Tsay, S. C.: Enhanced Deep Blue aerosol retrieval algorithm: The
858 second generation, *J Geophys Res-Atmos*, 118, 9296-9315, 10.1002/jgrd.50712,
859 2013.

860 Huneus, N., Schulz, M., Balkanski, Y., Griesfeller, J., Prospero, J., Kinne, S., Bauer, S.,
861 Boucher, O., Chin, M., Dentener, F., Diehl, T., Easter, R., Fillmore, D., Ghan, S.,
862 Ginoux, P., Grini, A., Horowitz, L., Koch, D., Krol, M. C., Landing, W., Liu, X.,
863 Mahowald, N., Miller, R., Morcrette, J. J., Myhre, G., Penner, J., Perlwitz, J.,
864 Stier, P., Takemura, T., and Zender, C. S.: Global dust model intercomparison in
865 AeroCom phase I, *Atmos Chem Phys*, 11, 7781-7816, 10.5194/acp-11-7781-
866 2011, 2011.

867 Jickells, T. D., An, Z. S., Andersen, K. K., Baker, A. R., Bergametti, G., Brooks, N., Cao,
868 J. J., Boyd, P. W., Duce, R. A., Hunter, K. A., Kawahata, H., Kubilay, N.,
869 laRoche, J., Liss, P. S., Mahowald, N., Prospero, J. M., Ridgwell, A. J., Tegen, I.,
870 and Torres, R.: Global iron connections between desert dust, ocean
871 biogeochemistry, and climate, *Science*, 308, 67-71, DOI
872 10.1126/science.1105959, 2005.

873 Jin, Q., Wei, J., Yang, Z. L., Pu, B., and Huang, J.: Consistent response of Indian summer
874 monsoon to Middle East dust in observations and simulations, *Atmos Chem Phys*,
875 15, 9897-9915, 10.5194/acp-15-9897-2015, 2015.

876 Jin, Q. J., Wei, J. F., and Yang, Z. L.: Positive response of Indian summer rainfall to
877 Middle East dust, *Geophys Res Lett*, 41, 4068-4074, 10.1002/2014gl059980,
878 2014.

879 Jin, Q. J., Yang, Z. L., and Wei, J. F.: Seasonal Responses of Indian Summer Monsoon to
880 Dust Aerosols in the Middle East, India, and China, *J Climate*, 29, 6329-6349,
881 10.1175/Jcli-D-15-0622.1, 2016.

882 Kim, M. K., Lau, W. K. M., Kim, K. M., Sang, J., Kim, Y. H., and Lee, W. S.:
883 Amplification of ENSO effects on Indian summer monsoon by absorbing
884 aerosols, *Clim Dynam*, 46, 2657-2671, 10.1007/s00382-015-2722-y, 2016.

885 Kok, J. F., Ridley, D. A., Zhou, Q., Miller, R. L., Zhao, C., Heald, C. L., Ward, D. S.,
886 Albani, S., and Haustein, K.: Smaller desert dust cooling effect estimated from
887 analysis of dust size and abundance, *Nat Geosci*, 10, 274+, 10.1038/Ngeo2912,
888 2017.

889 Laurent, B., Marticorena, B., Bergametti, G., and Mei, F.: Modeling mineral dust
890 emissions from Chinese and Mongolian deserts, *Global Planet Change*, 52, 121-
891 141, 10.1016/j.gloplacha.2006.02.012, 2006.

892 Levin, Z., Ganor, E., and Gladstein, V.: The effects of desert particles coated with sulfate
893 on rain formation in the eastern Mediterranean, *J Appl Meteorol*, 35, 1511-1523,
894 Doi 10.1175/1520-0450(1996)035<1511:Teodpc>2.0.Co;2, 1996.

895 Mahowald, N. M., and Luo, C.: A less dusty future?, *Geophys Res Lett*, 30,
896 10.1029/2003gl017880, 2003.

897 Mahowald, N. M., Kloster, S., Engelstaedter, S., Moore, J. K., Mukhopadhyay, S.,
898 McConnell, J. R., Albani, S., Doney, S. C., Bhattacharya, A., Curran, M. A. J.,
899 Flanner, M. G., Hoffman, F. M., Lawrence, D. M., Lindsay, K., Mayewski, P. A.,
900 Neff, J., Rothenberg, D., Thomas, E., Thornton, P. E., and Zender, C. S.:
901 Observed 20th century desert dust variability: impact on climate and
902 biogeochemistry, *Atmos Chem Phys*, 10, 10875-10893, 10.5194/acp-10-10875-
903 2010, 2010.

904 Marticorena, B., and Bergametti, G.: Modeling the Atmospheric Dust Cycle .1. Design of
905 a Soil-Derived Dust Emission Scheme, *J Geophys Res-Atmos*, 100, 16415-16430,
906 Doi 10.1029/95jd00690, 1995.

907 Marx, S. K., McGowan, H. A., and Kamber, B. S.: Long-range dust transport from
908 eastern Australia: A proxy for Holocene aridity and ENSO-type climate
909 variability, *Earth Planet Sc Lett*, 282, 167-177, 10.1016/j.epsl.2009.03.013, 2009.

910 McConnell, J. R., Aristarain, A. J., Banta, J. R., Edwards, P. R., and Simoes, J. C.: 20th-
911 Century doubling in dust archived in an Antarctic Peninsula ice core parallels

912 climate change and desertification in South America, *P Natl Acad Sci USA*, 104,
913 5743-5748, 10.1073/pnas.0607657104, 2007.

914 Miller, R. L., and Tegen, I.: Climate response to soil dust aerosols, *J Climate*, 11, 3247-
915 3267, Doi 10.1175/1520-0442(1998)011<3247:Crtsda>2.0.Co;2, 1998.

916 Miller, R. L., Tegen, I., and Perlwitz, J.: Surface radiative forcing by soil dust aerosols
917 and the hydrologic cycle, *J Geophys Res-Atmos*, 109, 10.1029/2003jd004085,
918 2004.

919 Misra, A., Kanawade, V. P., and Tripathi, S. N.: Quantitative assessment of AOD from
920 17 CMIP5 models based on satellite-derived AOD over India, *Ann Geophys-*
921 *Germany*, 34, 657-671, 10.5194/angeo-34-657-2016, 2016.

922 Moulin, C., and Chiapello, I.: Impact of human-induced desertification on the
923 intensification of Sahel dust emission and export over the last decades, *Geophys*
924 *Res Lett*, 33, 10.1029/2006gl025923, 2006.

925 Myhre, G., Shindell, D., Bréon, F.-M., Collins, W., Fuglestvedt, J., Huang, J., Koch, D.,
926 Lamarque, J.-F., Lee, D., Mendoza, B., Nakajima, T., Robock, A., Stephens, G.,
927 Takemura, T., and Zhang, H.: Anthropogenic and Natural Radiative Forcing. , in:
928 *Climate Change 2013: The Physical Science Basis. Contribution of Working*
929 *Group I to the Fifth Assessment Report of the Intergovernmental Panel on*
930 *Climate Change*, edited by: Stocker, T. F., Qin, D., Plattner, G.-K., Tignor, M.,
931 Allen, S. K., Boschung, J., Nauels, A., Xia, Y., Bex, V., and Midgley, P. M.,
932 Cambridge University Press, Cambridge, United Kingdom and New York, NY,
933 USA, 2013.

934 Nakajima, T., Higurashi, A., Kawamoto, K., and Penner, J. E.: A possible correlation
935 between satellite-derived cloud and aerosol microphysical parameters, *Geophys*
936 *Res Lett*, 28, 1171-1174, Doi 10.1029/2000gl012186, 2001.

937 Neff, J. C., Reynolds, R. L., Belnap, J., and Lamothe, P.: Multi-decadal impacts of
938 grazing on soil physical and biogeochemical properties in southeast Utah, *Ecol*
939 *Appl*, 15, 87-95, Doi 10.1890/04-0268, 2005.

940 Neff, J. C., Ballantyne, A. P., Farmer, G. L., Mahowald, N. M., Conroy, J. L., Landry, C.
941 C., Overpeck, J. T., Painter, T. H., Lawrence, C. R., and Reynolds, R. L.:
942 Increasing eolian dust deposition in the western United States linked to human
943 activity, *Nat Geosci*, 1, 189-195, 10.1038/ngeo133, 2008.

944 O'Brien, R. M.: A caution regarding rules of thumb for variance inflation factors, *Qual*
945 *Quant*, 41, 673-690, 10.1007/s11135-006-9018-6, 2007.

946 O'Neill, N. T., Eck, T. F., Smirnov, A., Holben, B. N., and Thulasiraman, S.: Spectral
947 discrimination of coarse and fine mode optical depth, *J Geophys Res-Atmos*, 108,
948 10.1029/2002jd002975, 2003.

949 Prospero, J. M., and Nees, R. T.: Impact of the North African Drought and El-Nino on
950 Mineral Dust in the Barbados Trade Winds, *Nature*, 320, 735-738, DOI
951 10.1038/320735a0, 1986.

952 Prospero, J. M., and Lamb, P. J.: African droughts and dust transport to the Caribbean:
953 Climate change implications, *Science*, 302, 1024-1027, DOI
954 10.1126/science.1089915, 2003.

955 Pu, B., Fu, R., Dickinson, R. E., and Fernando, D. N.: Why do summer droughts in the
956 Southern Great Plains occur in some La Nina years but not others?, *J Geophys*
957 *Res-Atmos*, 121, 1120-1137, 10.1002/2015jd023508, 2016.

958 Pu, B., and Ginoux, P.: The impact of the Pacific Decadal Oscillation on springtime dust
959 activity in Syria, *Atmos Chem Phys*, 16, 13431-13448, 10.5194/acp-16-13431-
960 2016, 2016.

961 Pu, B., and Ginoux, P.: Projection of American dustiness in the late 21st century due to
962 climate change, *Scientific reports*, 7, 10.1038/s41598-017-05431-9, 2017.

963 Reader, M. C., Fung, I., and McFarlane, N.: The mineral dust aerosol cycle during the
964 last glacial maximum (vol 104, pg 9381, 1999), *J Geophys Res-Atmos*, 104,
965 22319-22320, Doi 10.1029/1999jd900434, 1999.

966 Riahi, K., Rao, S., Krey, V., Cho, C. H., Chirkov, V., Fischer, G., Kindermann, G.,
967 Nakicenovic, N., and Rafaj, P.: RCP 8.5-A scenario of comparatively high
968 greenhouse gas emissions, *Climatic Change*, 109, 33-57, 10.1007/s10584-011-
969 0149-y, 2011.

970 Rosenfield, J. E., Considine, D. B., Meade, P. E., Bacmeister, J. T., Jackman, C. H., and
971 Schoeberl, M. R.: Stratospheric effects of Mount Pinatubo aerosol studied with a
972 coupled two-dimensional model, *J Geophys Res-Atmos*, 102, 3649-3670, Doi
973 10.1029/96jd03820, 1997.

974 Sanap, S. D., Ayantika, D. C., Pandithurai, G., and Niranjana, K.: Assessment of the
975 aerosol distribution over Indian subcontinent in CMIP5 models, *Atmospheric*
976 *Environment*, 87, 123-137, 10.1016/j.atmosenv.2014.01.017, 2014.

977 Seland, O., Iversen, T., Kirkevåg, A., and Storelvmo, T.: Aerosol-climate interactions in
978 the CAM-Oslo atmospheric GCM and investigation of associated basic
979 shortcomings, *Tellus A*, 60, 459-491, 10.1111/j.1600-0870.2008.00318.x, 2008.

980 Shao, Y. P., Wyrwoll, K. H., Chappell, A., Huang, J. P., Lin, Z. H., McTainsh, G. H.,
981 Mikami, M., Tanaka, T. Y., Wang, X. L., and Yoon, S.: Dust cycle: An emerging
982 core theme in Earth system science, *Aeolian Res*, 2, 181-204,
983 10.1016/j.aeolia.2011.02.001, 2011.

984 Sharma, D., and Miller, R. L.: Revisiting the observed correlation between weekly
985 averaged Indian monsoon precipitation and Arabian Sea aerosol optical depth,
986 *Geophys Res Lett*, 44, 10006-10016, 10.1002/2017gl074373, 2017.

987 Shindell, D. T., Lamarque, J. F., Schulz, M., Flanner, M., Jiao, C., Chin, M., Young, P. J.,
988 Lee, Y. H., Rotstayn, L., Mahowald, N., Milly, G., Faluvegi, G., Balkanski, Y.,
989 Collins, W. J., Conley, A. J., Dalsoren, S., Easter, R., Ghan, S., Horowitz, L., Liu,
990 X., Myhre, G., Nagashima, T., Naik, V., Rumbold, S. T., Skeie, R., Sudo, K.,
991 Szopa, S., Takemura, T., Voulgarakis, A., Yoon, J. H., and Lo, F.: Radiative
992 forcing in the ACCMIP historical and future climate simulations, *Atmos Chem*
993 *Phys*, 13, 2939-2974, 10.5194/acp-13-2939-2013, 2013.

994 Solmon, F., Nair, V. S., and Mallet, M.: Increasing Arabian dust activity and the Indian
995 summer monsoon, *Atmos Chem Phys*, 15, 8051-8064, 10.5194/acp-15-8051-
996 2015, 2015.

997 Strong, J. D., Vecchi, G. A., and Ginoux, P.: The Climatological Effect of Saharan Dust
998 on Global Tropical Cyclones in a Fully Coupled GCM, *Journal of Geophysical*
999 *Research - Atmospheres*, 123, <https://doi.org/10.1029/2017JD027808>, 2018.

1000 Strong, J. D. O., Vecchi, G. A., and Ginoux, P.: The Response of the Tropical Atlantic
1001 and West African Climate to Saharan Dust in a Fully Coupled GCM, *J Climate*,
1002 28, 7071-7092, 10.1175/Jcli-D-14-00797.1, 2015.

1003 Sun, D. L., Lau, K. M., and Kafatos, M.: Contrasting the 2007 and 2005 hurricane
1004 seasons: Evidence of possible impacts of Saharan dry air and dust on tropical
1005 cyclone activity in the Atlantic basin, *Geophys Res Lett*, 35,
1006 10.1029/2008gl034529, 2008.

1007 Takemura, T., Okamoto, H., Maruyama, Y., Numaguti, A., Higurashi, A., and Nakajima,
1008 T.: Global three-dimensional simulation of aerosol optical thickness distribution
1009 of various origins, *J Geophys Res-Atmos*, 105, 17853-17873, Doi
1010 10.1029/2000jd900265, 2000.

1011 Tegen, I., Harrison, S. P., Kohfeld, K., Prentice, I. C., Coe, M., and Heimann, M.: Impact
1012 of vegetation and preferential source areas on global dust aerosol: Results from a
1013 model study, *J Geophys Res-Atmos*, 107, 10.1029/2001jd000963, 2002.

1014 Tegen, I., Werner, M., Harrison, S. P., and Kohfeld, K. E.: Relative importance of
1015 climate and land use in determining present and future global soil dust emission,
1016 *Geophys Res Lett*, 31, 10.1029/2003gl019216, 2004.

1017 Todd, M. C., Washington, R., Raghavan, S., Lizcano, G., and Knippertz, P.: Regional
1018 model simulations of the Bodele low-level jet of northern Chad during the Bodele
1019 Dust Experiment (BoDEX 2005), *J Climate*, 21, 995-1012,
1020 10.1175/2007jcli1766.1, 2008.

1021 Vinoj, V., Rasch, P. J., Wang, H. L., Yoon, J. H., Ma, P. L., Landu, K., and Singh, B.:
1022 Short-term modulation of Indian summer monsoon rainfall by West Asian dust,
1023 Nat Geosci, 7, 308-313, 10.1038/ngeo2107, 2014.

1024 Watanabe, S., Hajima, T., Sudo, K., Nagashima, T., Takemura, T., Okajima, H., Nozawa,
1025 T., Kawase, H., Abe, M., Yokohata, T., Ise, T., Sato, H., Kato, E., Takata, K.,
1026 Emori, S., and Kawamiya, M.: MIROC-ESM 2010: model description and basic
1027 results of CMIP5-20c3m experiments, Geosci Model Dev, 4, 845-872,
1028 10.5194/gmd-4-845-2011, 2011.

1029 Winker, D. M., Hunt, W., and Hostetler, C.: Status and performance of the CALIOP
1030 lidar, Bba Lib, 5575, 8-15, 10.1117/12.571955, 2004.

1031 Winker, D. M., Hunt, W. H., and McGill, M. J.: Initial performance assessment of
1032 CALIOP, Geophys Res Lett, 34, 10.1029/2007gl030135, 2007.

1033 Wong, S., and Dessler, A. E.: Suppression of deep convection over the tropical North
1034 Atlantic by the Saharan Air Layer, Geophys Res Lett, 32, 10.1029/2004gl022295,
1035 2005.

1036 Wurzler, S., Reisin, T. G., and Levin, Z.: Modification of mineral dust particles by cloud
1037 processing and subsequent effects on drop size distributions, J Geophys Res-
1038 Atmos, 105, 4501-4512, Doi 10.1029/1999jd900980, 2000.

1039 Zender, C. S., and Kwon, E. Y.: Regional contrasts in dust emission responses to climate,
1040 J Geophys Res-Atmos, 110, 10.1029/2004jd005501, 2005.

1041 Zhao, T. L., Gong, S. L., Zhang, X. Y., Blanchet, J. P., McKendry, I. G., and Zhou, Z. J.:
1042 A simulated climatology of Asian dust aerosol and its trans-Pacific transport. Part

1043 I: Mean climate and validation, J Climate, 19, 88-103, Doi 10.1175/Jcli3605.1,
1044 2006.
1045
1046
1047

1048 Table 1 CMIP5 models used in this study. Models tagged with plus signs (+) **considered**
1049 **included** anthropogenic land use/land cover change in their vegetation prediction.

1050

1051 Table 2 List of regions selected to compare model output with MODIS DOD. Locations of these
1052 regions are also plotted in Fig. 1b. Acronyms are used for some regions for short, and are listed
1053 in the brackets in the first column. Note that the region names such as Northern China and India
1054 are not exactly the same as their geographical definitions but also covers some areas from
1055 nearby countries.

1056

1057 Table 3 Changes of DOD in the late half of the 21st century (2051-2100; RCP 8.5 scenario) from
1058 the historical condition (1861-2005) projected by CMIP5 multi-model mean (second to fifth
1059 columns) and the regression model (sixth to ninth columns) in the nine regions. Changes of
1060 DOD are shown in percentage with reference to CMIP5 multi-model historical run. Note that in
1061 some regions the projected change by the regression model is quite large (i.e., greater than \pm
1062 100%), largely due to the underestimation of CMIP5 historical run in these regions.

1063

1064

1065

1066

1067

1068

1069

1070

1071

1072

1073 Figure 1. Figure 1. Climatology (2004-2016) of Aqua and Terra combined DOD (i.e., MODIS
1074 DOD; top panel) and multi-model mean of CMIP5 DOD (bottom) for four seasons. The pattern
1075 correlation (centered; calculated after interpolating ~~MODIS~~-MODIS DOD to CMIP5 DOD
1076 grids) between CMIP5 and MODIS DOD are shown in pink in the bottom panel. Blue numbers
1077 denote global mean DOD over land. For CMIP5 model results, \pm one standard deviation among
1078 seven CMIP5 models is also shown. Black boxes in (b) denote nine averaging regions (Table 2).
1079 Here we only added these boxes in (b) instead of every plot to keep the figure clean. Note that
1080 CMIP5 multi-model mean is masked by MODIS DOD for comparison. Dotted area in (e)-(h)
1081 shows where multi-model mean is greater than one inter-model standard deviation.

1082

1083 Figure 2. Zonal mean DOD from MODIS (thick red), CMIP5 multi-model mean (thick black),
1084 and each individual model (other colorful lines).

1085

1086 Figure 3. Seasonal cycle of DOD in nine regions (Table 2) averaged over 2004-2016. Thick red
1087 lines denote MODIS DOD, thick black lines denote CMIP5 multi-model mean, and other
1088 colorful lines denote individual model output. The annual means from MODIS DOD (Obs; red)

1089 and multi-model mean (Ens; black) are shown- in each panel. Note that in (i) MODIS DOD (red

1090 line) is scaled ten times to better display the season cycle.

1091

1092 Figure 4. Spatial statistics comparing DOD from CMIP5 models with that from MODIS in nine
1093 regions. Label on the X-axis shows individual models (1-7) and multi-model mean (8). Y-axis
1094 shows the ratio of pattern standard deviations between model climatology (2004-2016) and that
1095 of MODIS, which reveals the relative amplitude of the simulated DOD versus satellite DOD.
1096 The color denotes pattern correlation (centered) between each model and MODIS DOD in each
1097 region.

1098

1099 Figure 5. Correlations (color) between regional averaged time series from CMIP5 DOD and
1100 MODIS DOD from 2004 to 2016 for four seasons. Numbers in the X-axis denotes each model
1101 (1-7) and multi-model mean (8). Correlations significant at the 90% confidence level are
1102 marked by a star and significance at the 95% confidence level by two stars.

1103

1104 Figure 6. Regression coefficients calculated by regressing DOD in each season onto
1105 standardized precipitation (purple), bareness (orange), and surface wind speed (green) from
1106 2004 to 2016. Coefficients obtained using MODIS DOD and observed controlling factors
1107 (interpolated to a 2° by 2.5° grid) and those using CMIP5 multi-model mean DOD and
1108 controlling factors are shown in the left and right columns, respectively. The color of the
1109 shading denotes the largest coefficient in absolute value among the three, while the saturation of
1110 the color shows the magnitude of the coefficient (from 0 to 0.02). Only regression coefficients
1111 significant at the 90% confidence level (Bootstrap test) are shown. Missing values are shaded in
1112 grey. To highlight coefficients near the source regions, a mask of $LAI \leq 0.5$ is applied.

1113

1114 Figure 7. Projected changes of DOD in the late half of the 21st century (under the RCP 8.5
1115 scenario) from that in the historical level (1861-2005) by CMIP5 multi-model mean for four
1116 seasons. The percentage change of global mean (over land) DOD \pm one inter-model standard
1117 deviation is shown at the bottom of each plot. Areas with sign agreement among the models
1118 reaches 71.4% (i.e., at least five out of seven models have the same sign as the multi-model
1119 mean) are dotted. ~~one inter-among the models reaches 71.4% (i.e., at least five out seven~~
1120 ~~models have the same sign as the multi-model mean) are dotted.~~

1121

1122 Figure 8. Projected difference of (a)-(d) precipitation (mm day⁻¹), (e)-(h) bareness, and (i)-(l) 10
1123 m wind (m s⁻¹) between the late half of the 21st century (2051-2100; RCP 8.5 scenario) and
1124 historical level (1861-2005) from multi-model mean of seven CMIP5 models. Areas with sign
1125 agreement among the models reaches 71.4% (i.e., at least five out of seven models have the
1126 same sign as the multi-model mean) are dotted.

1127

1128 Figure 9. Projected change of DOD in the late half of the 21st century under the RCP 8.5
1129 scenario by the regression model. The results are calculated using the regression coefficients
1130 obtained from observations during 2004-2016 (see methodology) and projected changes of
1131 precipitation, bareness, and surface wind from ~~seven+6~~ CMIP5 models. Dotted areas are
1132 regions with sign agreement among the regression projections (using output of each of the seven
1133 models) above 71.4% (i.e., at least five out of seven regression projections have the same sign
1134 as the multi-model mean projection). ~~Dotted areas are regions with sign agreement among the~~
1135 ~~models above 62.5% (i.e., at least 10 out 16 models have the same sign as the multi-model~~
1136 ~~mean).~~ To highlight DOD variations near the source regions, a mask of LAI ≤ 0.5 (from
1137 present-day climatology) is applied.

1138

1139 Figure 10. (a)-(d) Projected change of DOD in the late half of the 21st century under the RCP
1140 8.5 scenario by the regression model and output from seven CMIP5 models (same as Fig. 9),
1141 and contributions from each component, (e)-(h) precipitation, (j)-(i) bareness, and (m)-(p)
1142 surface wind speed. Dotted areas are regions with sign agreement among the models above
1143 ~~62.5~~71.4%. To highlight DOD variations near the source regions, a mask of LAI ≤ 0.5 (from
1144 present-day climatology) is applied.

1145

1146

1147 | Table 1 CMIP5 models used in this study. Models tagged with plus signs (+) **considered**
 1148 | **included** anthropogenic land use/land cover change in their vegetation prediction.
 1149 |

Model	lat/lon resolution	Dust emission implementation scheme	Dynamic Vegetation	Model reference
CanESM2	2.8°×2.8°	Reader et al. (1999); Croft et al. (2005)	N ⁺	Arora et al. (2011)
GFDL-CM3	2.0°×2.5°	Ginoux et al. (2001)	Y ⁺	Donner et al. (2011)
HadGEM2-CC	1.2°×1.8°	Marticorena and Bergametti (1995)	Y ⁺	Collins et al. (2011)
HadGEM2-ES	1.2°×1.8°	Marticorena and Bergametti (1995)	Y ⁺	Collins et al. (2011)
MIROC-ESM	2.8°×2.8°	Takemura et al. (2000)	Y ⁺	Watanabe et al. (2011)
MIROC-ESM-CHEM	2.8°×2.8°	Takemura et al. (2000)	Y ⁺	Watanabe et al. (2011)
NorESM1-M	1.9°×2.5°	Seland et al. (2008)	N ⁺	Bentsen et al. (2013)

1150
 1151
 1152
 1153
 1154
 1155
 1156
 1157
 1158
 1159
 1160
 1161
 1162
 1163
 1164
 1165
 1166
 1167
 1168
 1169
 1170
 1171
 1172
 1173
 1174
 1175
 1176
 1177
 1178
 1179
 1180
 1181
 1182

1183 Table 2 List of regions selected to compare model output with MODIS DOD. Locations of these
 1184 regions are also plotted in Fig. 1b. Acronyms are used for some regions for short, and are listed
 1185 in the brackets in the first column. Note that the region names such as Northern China and
 1186 India are not exactly the same as their geographical definitions but also covers some areas from
 1187 nearby countries.
 1188

Region	Domain
North Africa (N. Africa)	5°-50°N, 18°W-35°E
Middle East	12°-50°N, 35°-60°E
Northern China (N. China)	35°-50°N, 70°-110°E
North America (N. America)	25°-50°N, 95°-125°W
India	5°-35°N, 60°-90°E
Southeastern Asia (SE. Asia)	9°-35°N, 90°-121°E
South Africa (S. Africa)	15°-35°S, 10°-50°E
South America (S. America)	0°-55°S, 60°-83°W
Australia	10°-40°S, 112°-155°E

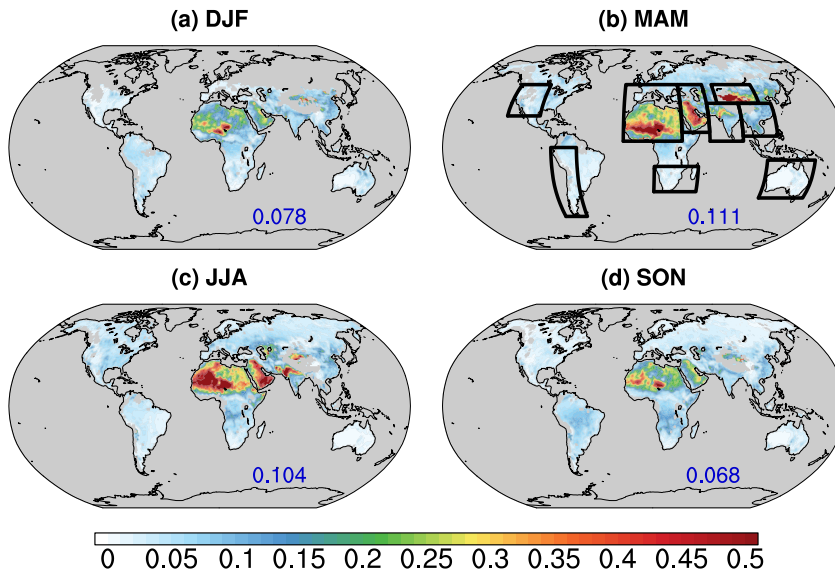
1189
 1190
 1191
 1192
 1193
 1194
 1195
 1196
 1197
 1198
 1199
 1200
 1201
 1202
 1203
 1204
 1205
 1206
 1207
 1208
 1209
 1210
 1211
 1212
 1213
 1214
 1215
 1216
 1217
 1218
 1219
 1220

1221 Table 3 Changes of DOD in the late half of the 21st century (2051-2100; RCP 8.5 scenario) from
 1222 the historical condition (1861-2005) projected by CMIP5 multi-model mean (second to fifth
 1223 columns) and the regression model (sixth to ninth columns) in nine regions. Changes of DOD
 1224 are shown in percentage with reference to CMIP5 multi-model historical run. Note that in some
 1225 regions the projected change by the regression model is quite large (i.e., greater than $\pm 100\%$),
 1226 largely due to the underestimation of CMIP5 historical run in these regions.
 1227

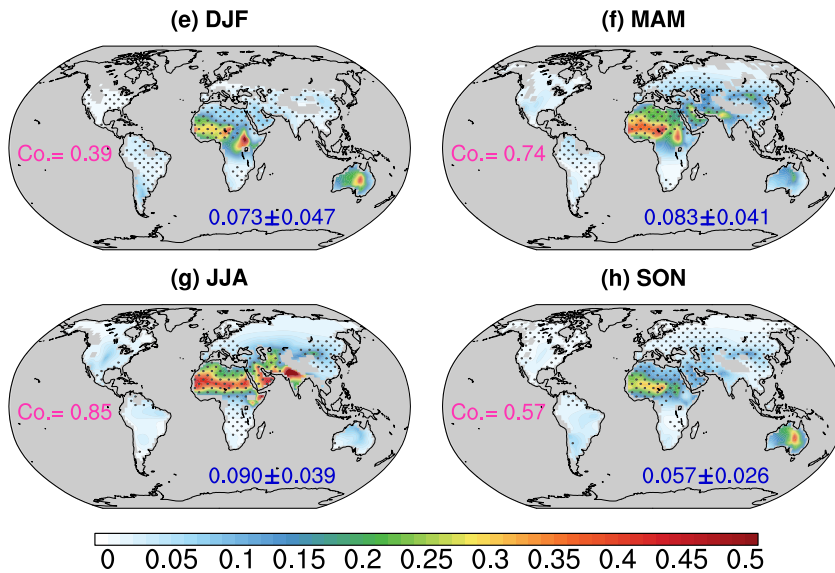
Region	CMIP5				Regression model			
	DJF	MAM	JJA	SON	DJF	MAM	JJA	SON
N. Africa	-3.8	-3.6	2.4	-16.3	-0.8	-17.7	11.1	-10.3
Middle East	7.8	4.5	6.4	1.5	9.8	-16.0	-5.4	-8.4
N. China	-33.5	-11.4	-9.8	-14.4	312.3	-238.6	-51.2	-30.0
N. America	42.6	26.8	13.2	-6.4	-38.5	-90.0	9.3	-42.4
India	-5.1	0.2	-1.0	-9.9	-27.6	-8.2	-2.9	-32.3
SE. Asia	-45.7	-16.5	-13.5	-17.1	-34.8	1.6	4.2	96.3
S. Africa	24.0	6.1	38.5	54.4	22.3	59.3	231.8	78.3
S. America	35.7	27.4	51.8	36.0	14.8	56.1	78.3	154.6
Australia	-3.2	-3.2	15.3	17.0	2.7	0.4	0.7	3.7

1228
 1229
 1230
 1231
 1232

MODIS DOD (2004-2016)



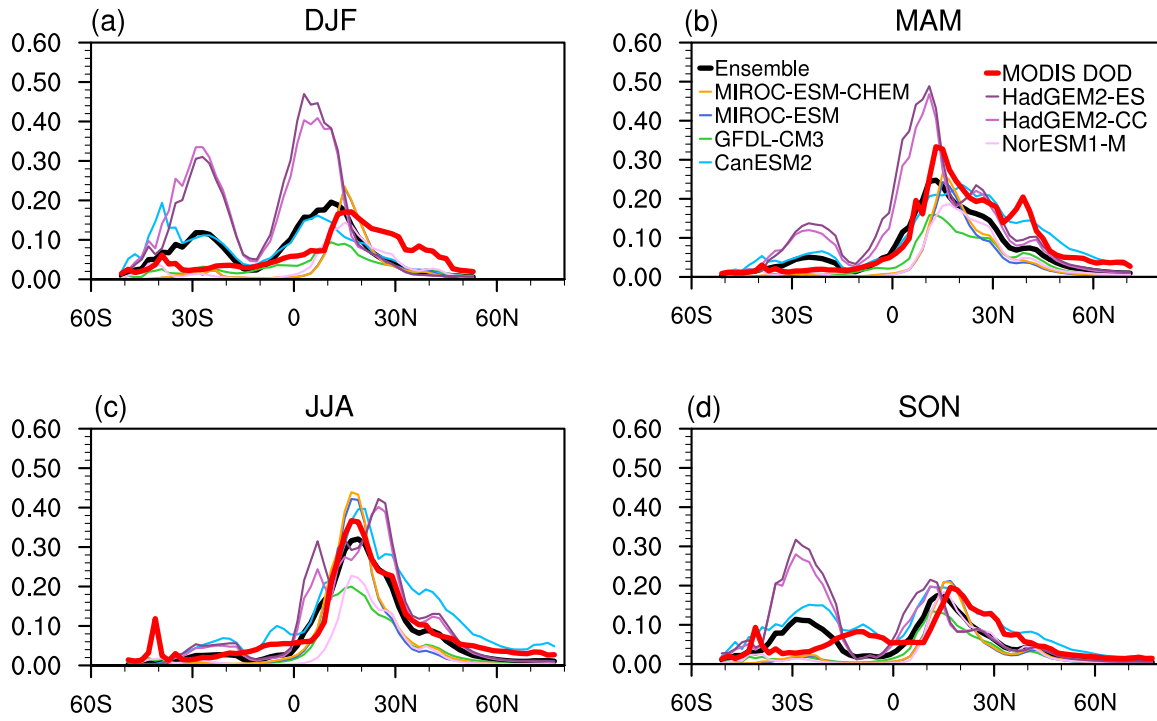
CMIP5 ensemble



1233
1234
1235
1236
1237
1238
1239
1240
1241
1242

Figure 1. Climatology (2004-2016) of Aqua and Terra combined DOD (i.e., MODIS DOD; top panel) and multi-model mean of CMIP5 DOD (bottom) for four seasons. The pattern correlation (centered; calculated after interpolating ~~MODIS-MODIS~~ DOD to CMIP5 DOD grids) between CMIP5 and MODIS DOD are shown in pink in the bottom panel. Blue numbers denote global mean DOD over land. For CMIP5 model results, \pm one standard deviation among seven CMIP5 models is also shown. Black boxes in (b) denote nine averaging regions (Table 2). Here we only added these boxes in (b) instead of every plot to keep the figure clean. Note that CMIP5 multi-model mean is masked by MODIS DOD for comparison. Dotted area in (e)-(h) shows where multi-model mean is greater than one inter-model standard deviation.

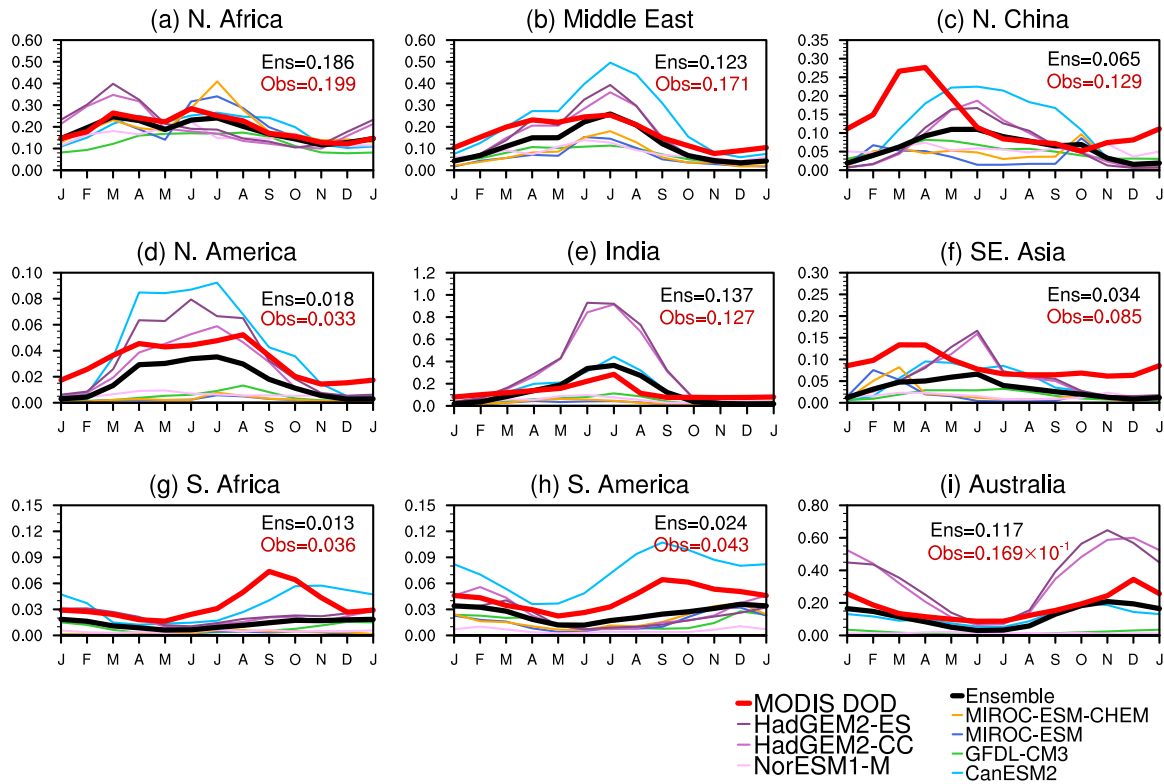
Zonal mean DOD



1243
1244
1245
1246
1247
1248
1249
1250
1251
1252
1253
1254
1255
1256
1257
1258
1259
1260
1261
1262
1263
1264
1265
1266
1267

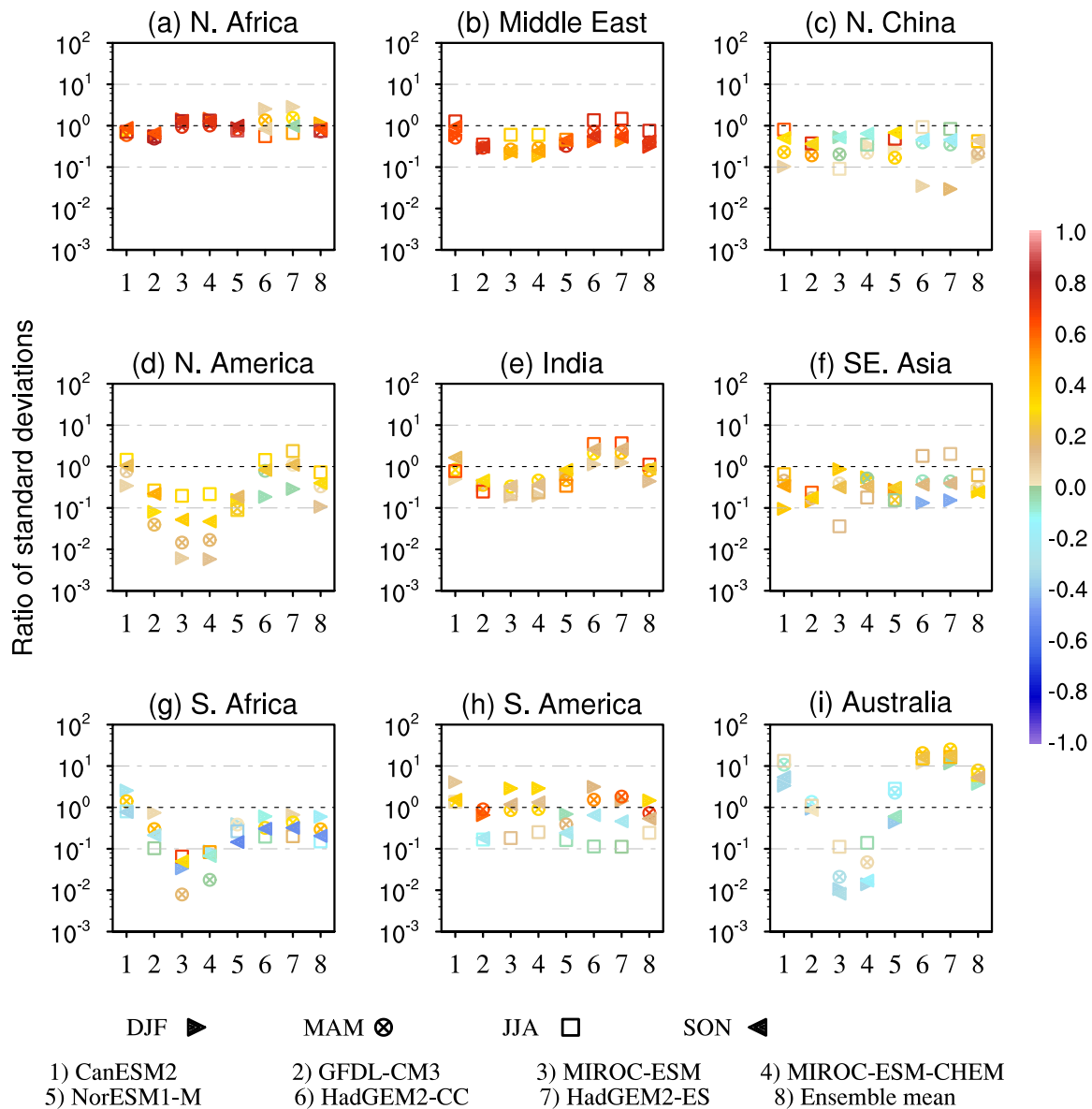
Figure 2. Zonal mean DOD from MODIS (thick red), CMIP5 multi-model mean (thick black), and each individual model (other colorful lines).

Dust optical depth (2004-2016)



1268
1269
1270
1271
1272
1273
1274
1275
1276
1277
1278
1279
1280
1281
1282
1283
1284
1285
1286
1287
1288
1289
1290
1291
1292

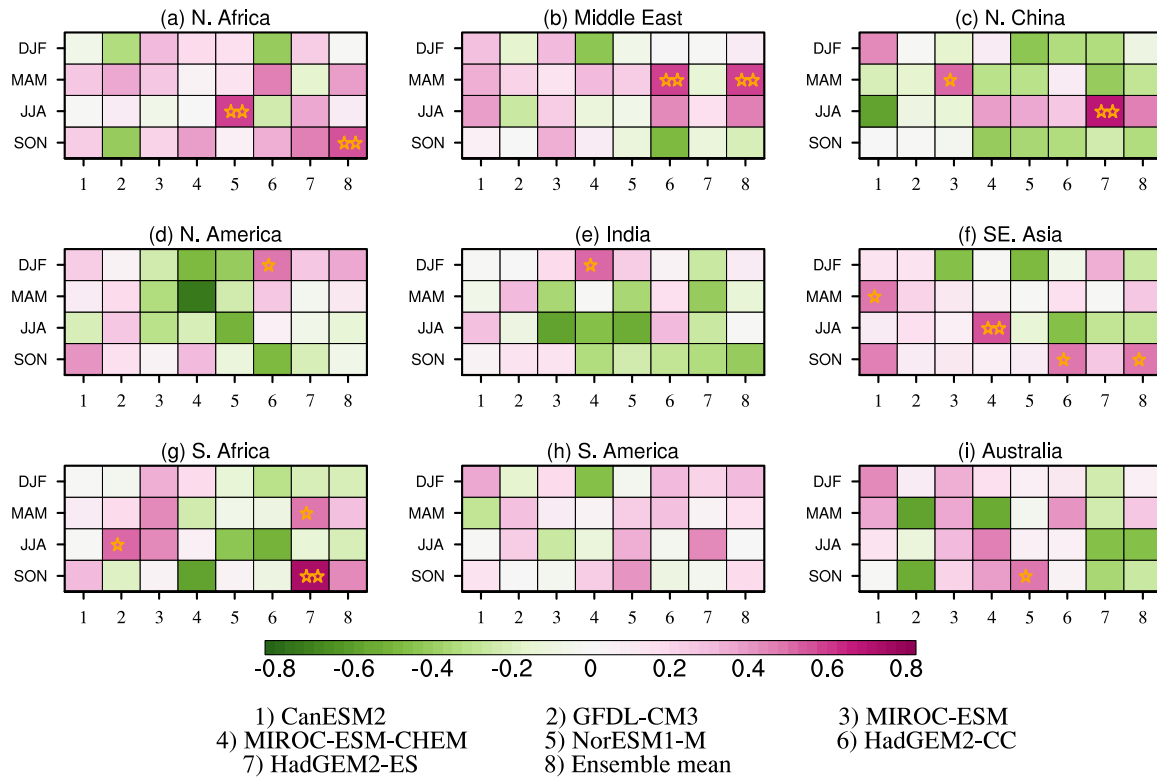
Figure 3. Seasonal cycle of DOD in nine regions (Table 2) averaged over 2004-2016. Thick red lines denote MODIS DOD, thick black lines denote CMIP5 multi-model mean, and other colorful lines denote individual model output. The annual means from MODIS DOD (Obs; red) and multi-model mean (Ens; black) are also listed in each panel. Note that in (i) MODIS DOD (red line) is scaled ten times to better display the season cycle.



1293
 1294
 1295
 1296
 1297
 1298
 1299
 1300
 1301
 1302
 1303
 1304
 1305
 1306
 1307

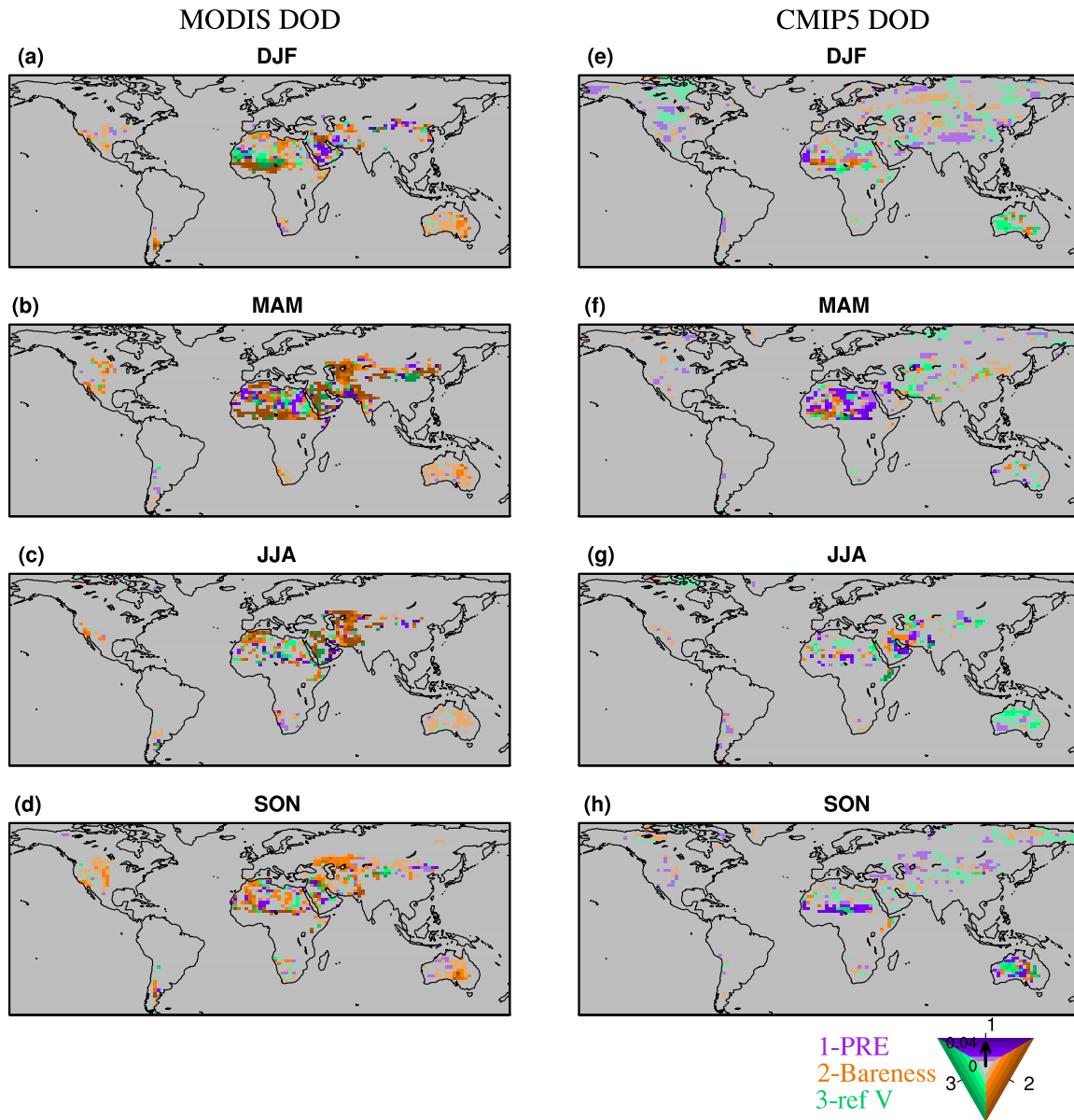
Figure 4. Spatial statistics comparing DOD from CMIP5 models with that from MODIS in nine regions. Label on the X-axis shows individual models (1-7) and multi-model mean (8). Y-axis shows the ratio of pattern standard deviations between model climatology (2004-2016) and that of MODIS, which reveals the relative amplitude of the simulated DOD versus satellite DOD. The color denotes pattern correlation (centered) between each model and MODIS DOD in each region.

DOD (CMIP5 vs. MODIS)



1308
 1309
 1310
 1311
 1312
 1313
 1314
 1315
 1316
 1317
 1318
 1319
 1320
 1321
 1322
 1323
 1324
 1325
 1326

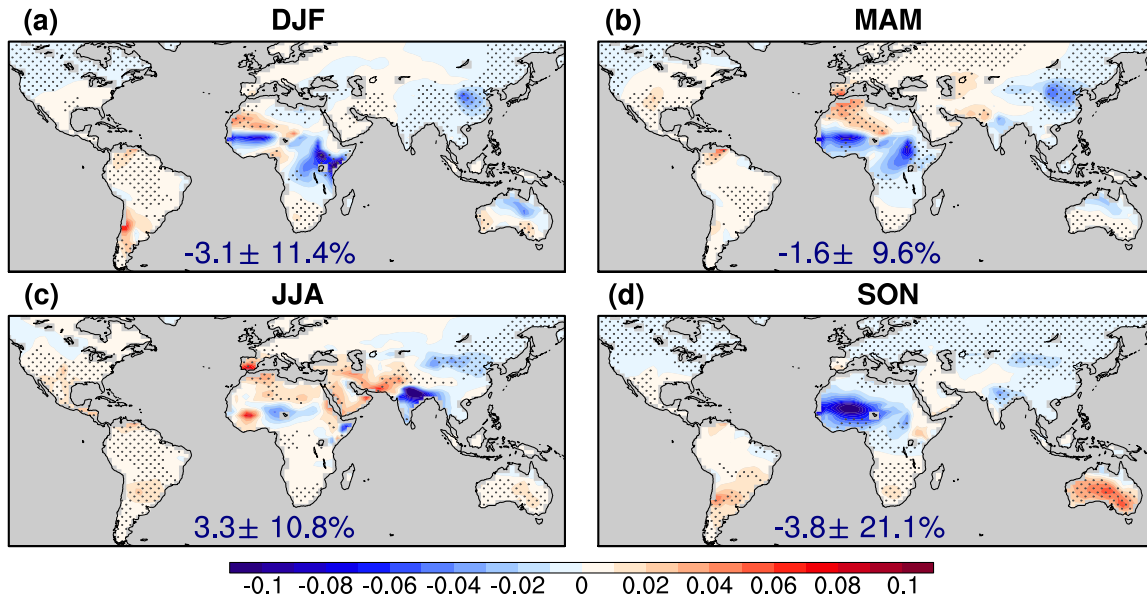
Figure 5. Correlations (color) between regional averaged time series from CMIP5 DOD and MODIS DOD from 2004 to 2016 for four seasons. Numbers in the X-axis denotes each model (1-7) and multi-model mean (8). Correlations significant at the 90% confidence level are marked by a star and significance at the 95% confidence level by two stars.



1327
 1328
 1329
 1330
 1331
 1332
 1333
 1334
 1335
 1336
 1337
 1338
 1339

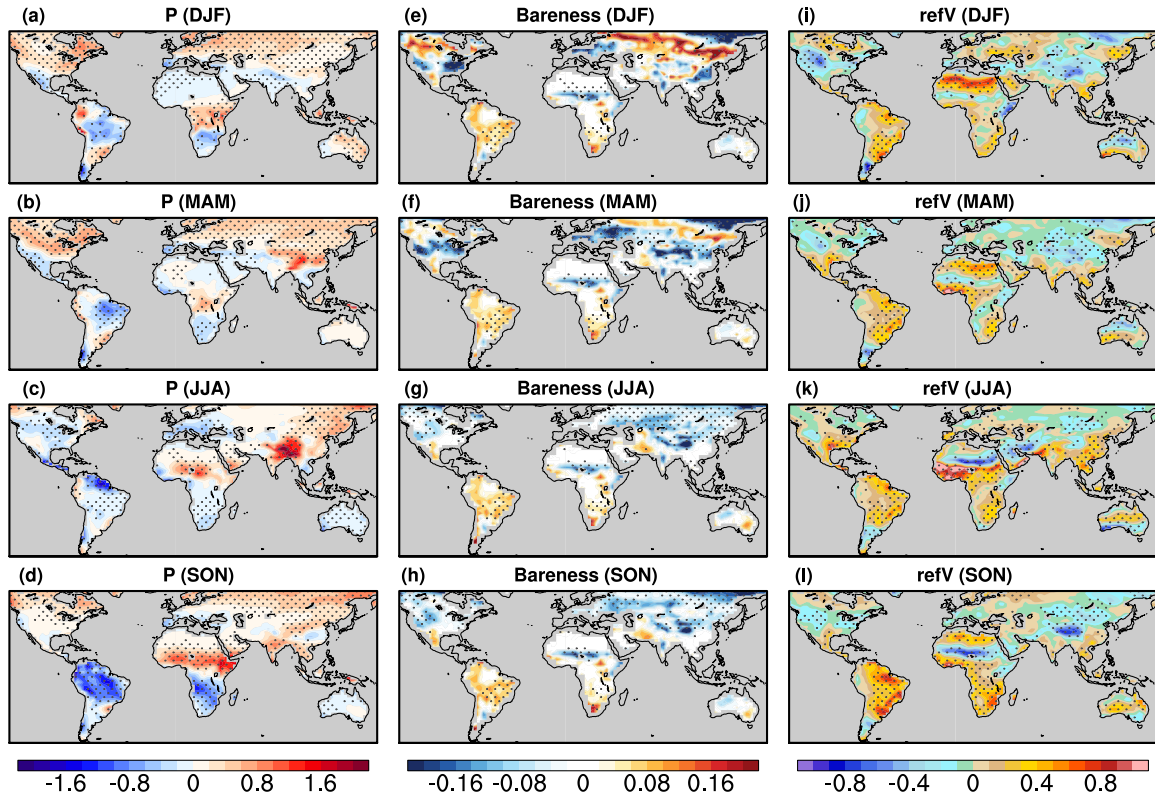
Figure 6. Regression coefficients calculated by regressing DOD in each season onto standardized precipitation (purple), bareness (orange), and surface wind speed (green) from 2004 to 2016. Coefficients obtained using MODIS DOD and observed controlling factors (interpolated to a 2° by 2.5° grid) and those using CMIP5 multi-model mean DOD and controlling factors are shown in the left and right columns, respectively. The color of the shading denotes the largest coefficient in absolute value among the three, while the saturation of the color shows the magnitude of the coefficient (from 0 to 0.042). Only regression coefficients significant at the 90% confidence level (Bootstrap test) are shown. Missing values are shaded in grey. To highlight coefficients near dust source regions, a mask of LAI ≤ 0.5 is applied.

Changes of CMIP5 DOD (2051-2100 minus 1861-2005)



1340
1341
1342
1343
1344
1345
1346
1347
1348
1349
1350
1351
1352
1353
1354
1355
1356
1357
1358
1359
1360
1361
1362
1363
1364
1365
1366
1367

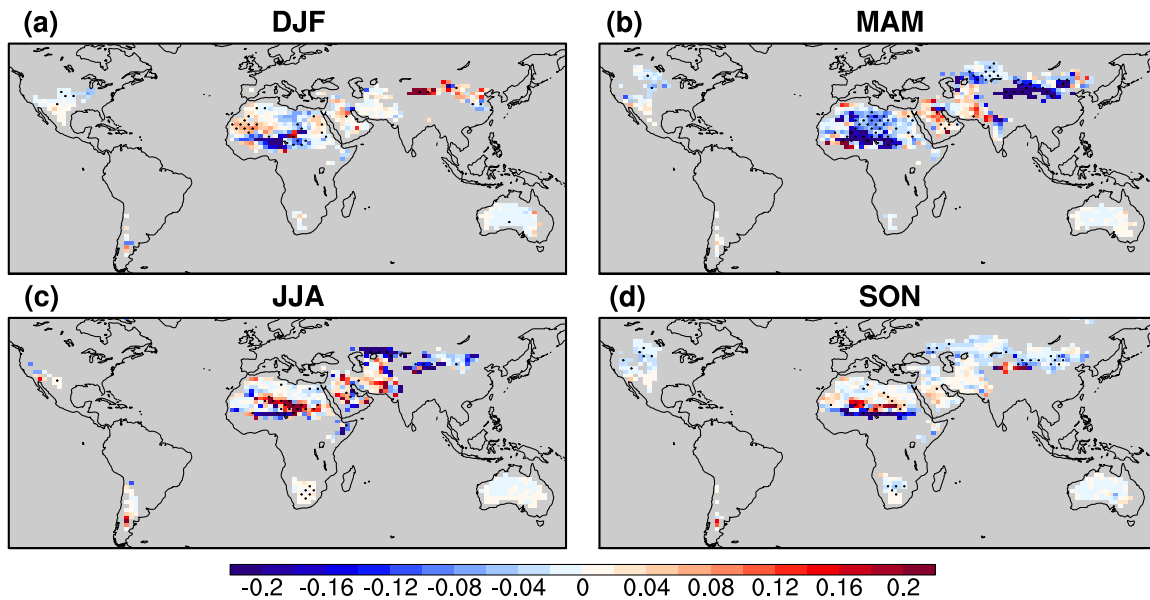
Figure 7. Projected changes of DOD in the late half of the 21st century (under the RCP 8.5 scenario) from that in the historical level (1861-2005) by CMIP5 multi-model mean for four seasons. The percentage change of global mean (over land) DOD \pm one inter-model standard deviation is shown at the bottom of each plot. Areas with sign agreement among the models reaches 71.4% (i.e., at least five out of seven models have the same sign as the multi-model mean) are dotted.



1368
 1369 Figure 8. Projected difference of (a)-(d) precipitation (mm day^{-1}), (e)-(h) bareness, and (i)-(l) 10
 1370 m wind (m s^{-1}) between the late half of the 21st century (2051-2100; RCP 8.5 scenario) and
 1371 historical level (1861-2005) from multi-model mean of seven CMIP5 models. Areas with sign
 1372 agreement among the models reaches 71.4% (i.e., at least five out of seven models have the
 1373 same sign as the multi-model mean) are dotted.

1374
 1375
 1376
 1377
 1378
 1379
 1380
 1381
 1382
 1383
 1384
 1385
 1386
 1387
 1388
 1389
 1390
 1391

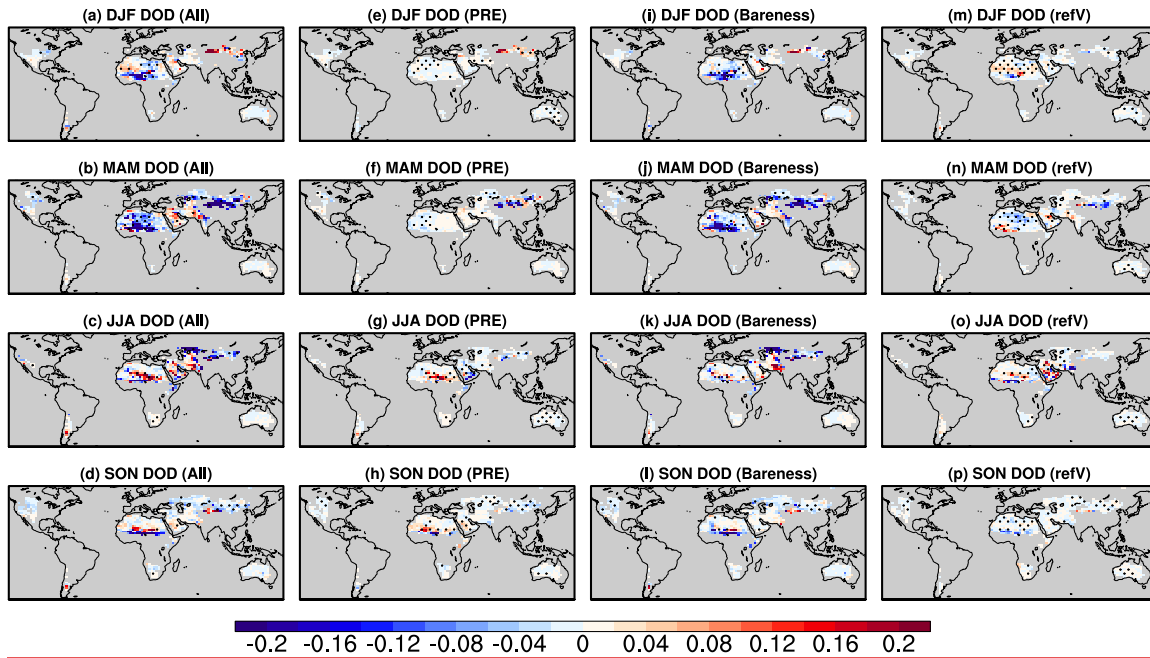
Changes of regDOD (2051-2100 minus 1861-2005)



1392
1393
1394
1395
1396
1397
1398
1399
1400
1401
1402
1403
1404
1405
1406
1407
1408
1409
1410
1411
1412
1413
1414
1415
1416
1417
1418
1419
1420
1421

Figure 9. Projected change of DOD in the late half of the 21st century under the RCP 8.5 scenario by the regression model. The results are calculated using the regression coefficients obtained from observations during 2004-2016 (see methodology) and projected changes of precipitation, bareness, and surface wind from ~~16~~seven CMIP5 models. Dotted areas are regions with sign agreement among the ~~models-regression projections~~ (using output of each of the seven models) above ~~62.5~~71.4% (i.e., at least ~~40~~five out of ~~seven~~16 ~~models-regression projections~~ projections have the same sign as the multi-model mean projection). To highlight DOD variations near the source regions, a mask of LAI ≤ 0.5 (from present-day climatology) is applied.

Changes of DOD (2051-2100 minus 1861-2005)



1422
1423
1424
1425
1426
1427
1428
1429

Figure 10. (a)-(d) Projected change of DOD in the late half of the 21st century under the RCP 8.5 scenario by the regression model and output from seven CMIP5 models (same as Fig. 9), and contributions from each component, (e)-(h) precipitation, (j)-(i) bareness, and (m)-(p) surface wind speed. Dotted areas are regions with sign agreement among the models-projections above 62.571.4%. To highlight DOD variations near the source regions, a mask of LAI ≤ 0.5 (from present-day climatology) is applied.